PHILOSOPHICAL TRANSACTIONS OF THE ROYAL SOCIETY A MATHEMATICAL, PHYSICAL & ENGINEERING SCIENCES

The Nucleation of Vorticity by Ions in Superfluid ^{4} He: I. Basic Theory

C. M. Muirhead, W. F. Vinen and R. J. Donnelly

Phil. Trans. R. Soc. Lond. A 1984 **311**, 433-467
doi: 10.1098/rsta.1984.0038

Phil. Trans. R. Soc. Lond. A **311**, 433–467 (1984) [433]
Printed in Great Britain

The nucleation of vorticity by ions in superfluid ^{4}He
I. Basic theory

By C. M. Muirhead[1], W. F. Vinen[1], F.R.S., and R. J. Donnelly[2]
[1] *Department of Physics, University of Birmingham, Birmingham B15 2TT, U.K.*
[2] *Department of Physics, University of Oregon, Eugene, Oregon* 97403, *U.S.A.*

(*Received* 19 *August* 1983)

CONTENTS

A theory is developed of vortex nucleation by an ion moving in superfluid helium at a low temperature. It is shown that production of a vortex loop attached to the side of the ion becomes energetically possible when the velocity of the ion exceeds a critical value, but that nucleation is impeded by the presence of a small potential barrier. The predicted critical velocity is close to that observed experimentally, at least at high pressure. Nucleation of an encircling vortex ring, considered some years ago by Schwarz & Jang (*Phys. Rev.* A **8**, 3199 (1973)), probably becomes possible only at a

higher velocity, and it is impeded by a large potential barrier. It is shown that for vortex loops the potential barrier can probably be overcome at a rate consistent with experiment either by quantum tunnelling at the lowest temperatures or thermally, by absorption of a single roton, at higher temperatures. Possible explanations of the recent observation by Bowley *et al.* (*Phil. Trans. R. Soc. Lond.* A**307**, 201 (1982)) that at high pressure the rate of vortex nucleation falls off at very high velocities are discussed.

1. Introduction

The experimental study of the motion of ions in superfluid ^{4}He has led to many interesting, instructive and important experimental results (see, for example, the review by Fetter (1976)). Both positive and negative ions can be formed in the liquid by means, for example, of a suitable radioactive source. The negative ion exists as a bare electron localized within an otherwise empty bubble, the bubble radius ranging from about 1.7 nm at the vapour pressure to about 1.15 nm near the melting pressure. The positive ion, He^+, exists at the centre of a sphere of solid helium, formed by electrostriction, with a radius of about 0.6 nm and with a large pressure gradient round the sphere. Both ions are therefore spherical structures, with sizes that are relatively large compared with an interatomic spacing, and both can move through the liquid under the influence, for example, of an electric field.

Suppose that an ion moves through superfluid ^{4}He at a low velocity. In its interaction with the superfluid component the ion will behave like a sphere moving through an ideal, inviscid, incompressible fluid; there will be no drag, but the effective mass of the sphere is increased by an amount equal to half the mass of the fluid displaced. Interaction with the normal fluid will arise from the scattering by the ion of the thermally excited quasi-particles (phonons and rotons) and any ^{3}He atoms in the liquid. These scattering processes will give rise to a drag on the ion and will therefore determine the low-field mobility of the ion. When the ion moves with high velocity, ideal superflow round the ion may break down. For ions at low pressures the breakdown involves the creation of quantized vortices (Rayfield & Reif 1964); for negative ions at higher pressure the breakdown may also involve the creation of rotons (Rayfield 1966, 1968; Phillips & McClintock 1974). Breakdown by the creation of rotons has been studied in great detail in the experiments of McClintock and his colleagues (Allum *et al.* 1977; Ellis *et al.* 1980); this process is interesting because it is the only known example of the breakdown of superflow by the mechanism originally discussed by Landau (1941). The creation of a quantized vortex by an ion seems usually to result in the formation of a vortex ring, in the core of which the ion becomes trapped; study of the resulting ion–vortex ring complex by Rayfield & Reif (1964) provided important confirmatory evidence for the existence of quantized vortices in superfluid helium.

It is generally believed that the creation of vortex line is the process by which ideal superflow usually breaks down in, for example, flow through a tube (see, for example, Vinen 1963). Vortex creation by a moving ion is therefore an example of a commonly occurring process in superfluid helium. However, the details of this type of process are not well understood: in particular, the the process by which the first short length of vortex line is formed (the nucleation process) is often obscure. Two factors contribute to this lack of understanding: flow through a tube, for example, often involves complicated end effects, which are difficult to disentangle; also, it seems likely that in practice the initial breakdown of ideal superflow is often caused by remnants of vortex line present before the flow is established (i.e. we are not dealing with an intrinsic nucleation process, which is the case of fundamental interest). These difficulties might be expected to be absent in

vortex nucleation by a moving ion: there seems no reason why an ion should have attached to it any nucleating remnant of vortex; and flow round an ion, at least at not too large a velocity, ought to be of simple dipolar form. A study of the nucleation of vorticity by a moving ion promises therefore to be important in contributing to our understanding of a process that is of considerable general importance in our understanding of superfluidity.

Many experiments have been reported that are of possible relevance to our study. We shall not attempt to review them at this stage, except to state that the critical velocity for the nucleation of vorticity by a moving ion is of order 40–60 m s^{-1}, and that the nucleation process appears to be stochastic in nature. Instead, we shall begin by exploring the nucleation problem theoretically; we shall introduce the experimental results at later stages when we can assess whether they are consistent with the theory.

It has long been recognized that vortex nucleation can usually take place only if the velocity of the relevant flow exceeds a critical value, and that even then the nucleation process will tend to be inhibited by a potential barrier (Vinen 1963). Our discussion must therefore aim to include, for the case of a moving ion, calculations of the critical velocity, of the shape and size of the potential barrier and of the rate at which this barrier can be overcome. There have been a number of earlier attempts to understand the nucleation of vorticity by a moving ion, and we shall refer particularly to those of Donnelly & Roberts (1971) and of Schwarz & Jang (1973); we believe, as we shall explain, that both contain elements of the truth, but that both are incomplete.

1.1. *Notation*

$\boldsymbol{A}$	vector potential (magnetic or hydrodynamic)
A	parameter of order unity occurring in equation (4.3.12)
a	interatomic spacing
a_0	effective radius of vortex core
$\boldsymbol{B}$	magnetic flux density
b	(§3.4) separation of vortex pair
b	(§4.2) parameter defining position of zero potential
$\tilde{b}$	spacing between vortex line and its image in an ion
C, C_{R}, C_{L}	correction factors for the energy of a vortex ring encircling an ion (equation (3.48)) (R for ring, L for loop)
d	thickness of helium film
$\mathrm{d}\tau$	element of volume
$\mathrm{d}\boldsymbol{l}$	element of length
$\boldsymbol{E}$	electric field
E_0	total hydrodynamic energy associated with a moving ion in the absence of vorticity
E_{c}	total hydrodynamic energy associated with a moving ion–vortex complex (c for complex)
$\mathscr{E}$	magnitude of electric field acting on an ion (§7.1)
$\mathscr{E}_{\mathrm{C}}$	magnitude of critical electric field acting on an ion (§7.1)
$g(\epsilon)$	density of quantum states associated with a vortex in a film
$\hbar$	the Planck constant divided by 2π
i	electric current (§3.1)
k_y, k'_y	wavenumber parameters entering the wavefunction for a vortex in a film

PHILOSOPHICAL TRANSACTIONS OF THE ROYAL SOCIETY A MATHEMATICAL, PHYSICAL & ENGINEERING SCIENCES

M_I effective mass of an ion
M_{Io} mass of bare ionic structure (Io for bare ion)
m effective mass per unit length of vortex core
m_c effective mass of vortex core
N number of ions (§7.1)
N_0 number of ions at time zero (§7.1)
n integer $\geqslant 0$
n_r number density of rotons
P pressure
$\boldsymbol{P}_0$ hydrodynamic impulse associated with a moving ion in the absence of vorticity
$\boldsymbol{P}_c$ hydrodynamic impulse associated with a moving ion–vortex complex
$\boldsymbol{P}_1$, $\boldsymbol{P}_2$, $\boldsymbol{P}_3$, $\boldsymbol{P}_4$ hydrodynamic impulses defined in §3.2
p magnitude of the hydrodynamic impulse associated with a vortex ring (or with unit length of a vortex pair) in an unbounded fluid
p_0 value of p in the limit $R/a_0 \gg 1$ (or $b/a_0 \gg 1$)
q electric charge per unit length (§4.1)
R radius of vortex ring in an unbounded fluid
R_I radius of ion
R_0 coordinate defining position of a vortex ring encircling an ion or a vortex loop attached to an ion.
$\tilde{R}$ radius of curvature of a vortex loop or ring
R_1, R_2 parameters describing observed vortex nucleation rate (§7.1)
r_0 radius of 'cyclotron orbit' associated with a vortex in a film (§4.2)
T temperature
$\boldsymbol{U}(U)$ velocity (speed) of sphere or ion through fluid or superfluid
$\boldsymbol{U}_s(U_s)$ superfluid velocity (speed) in a film
U_s' magnitude of effective superfluid velocity in a film (equation (4.3.2))
U_c magnitude of critical ionic velocity
$\bar{U}$ magnitude of mean ionic velocity
u_r, u_z, u_Z components of velocity of translation of vortex ring (§3.3)
$u(x)$ x-dependent part of vortex wavefunction ψ
V perturbation arising from interaction between helium film and bounding edge
V_c magnitude of critical mean ionic velocity
$\boldsymbol{v}$ fluid or superfluid velocity field
$\boldsymbol{v}_1$, $\boldsymbol{v}_2$ velocity fields defined in §3.2
v_y mean velocity of translation of vortex in y-direction in helium film
$\boldsymbol{v}_s$ superfluid velocity in a film
v_1, v_2, v_3 parameters describing observed vortex nucleation rate (§7.1)
w_0 width of potential barrier
x_0 coordinate describing mean position of vortex in film
Z_0 coordinate defining position of a vortex ring encircling an ion
Δ roton energy gap
ΔV effective potential energy of vortex in a film
$\Delta E_R(U, R_0, Z_0)$ change in energy $(E_c - E_0)$, at constant impulse, when a vortex ring forms round an ion (subscript R for ring)

PHILOSOPHICAL TRANSACTIONS OF THE ROYAL SOCIETY A MATHEMATICAL, PHYSICAL & ENGINEERING SCIENCES

$\Delta E_L(U, R_0, \theta_0)$ change in energy $(E_c - E_0)$, at constant impulse, when a vortex loop forms on an ion (subscript L for loop)
δ parameter in expression (3.4.1) for the energy of a vortex ring
ϵ energy of vortex ring (or per unit length of vortex pair) in an unbounded fluid
ϵ_0 value of ϵ in limit $R/a_0 \gg 1$ (or $b/a_0 \gg 1$)
θ_0 coordinate defining position of a vortex loop attached to an ion
$\boldsymbol{\kappa}(\kappa)$ circulation round a vortex regarded as a vector (scalar)
$\hat{\boldsymbol{\kappa}}$ $\boldsymbol{\kappa}/\kappa$
λ $R_1^2/(R_0^2 + Z_0^2)$
μ_0 permeability of free space
ν, ν_0 vortex nucleation rates (§4.3, §7.1)
$\bar{\nu}$ mean vortex nucleation rate (§7.1)
$\nu_s(\bar{\nu}_s), \nu_r(\bar{\nu}_r)$ temperature-independent and temperature-dependent components of $\nu(\bar{\nu})$
ρ_s superfluid density
τ relaxation time
ϕ velocity potential associated with velocity field $\boldsymbol{v}_2$
ψ wavefunction of vortex in a thin film
$\boldsymbol{\omega}$ vorticity

2. Approach and assumptions of the present treatment

In this paper we shall confine our attention to nucleation in pure ^{4}He. It is known from experiment that even small concentrations of ^{3}He can have a large effect on the nucleation process (Bowley *et al.* 1980), but we shall find it convenient to deal with this matter in a later paper. We shall assume, at least initially, that both positive and negative ions can be regarded as ideal smooth rigid spheres, and that flow of the superfluid in the neighbourhood of these spheres is, before nucleation, the same as that of an ideal continuous incompressible fluid. All these assumptions are of questionable validity, for the following reasons.

(i) The spheres are certainly not smooth on an atomic scale; this fact will turn out to be of potential importance when we consider vortex nucleation by quantum tunnelling (§4.3).

(ii) Around the ions there is a region of enhanced fluid density due to electrostriction.

(iii) As has been pointed out by Ellis *et al.* (1983), some distortion of the negative ion must probably occur at high velocity owing to a significant variation in the Bernoulli pressure over the surface of the bubble.

(iv) If the velocity of the sphere exceeds the Landau critical velocity for roton creation, the motion of the sphere is accompanied by the emission of a stream of rotons, roton emission occurring much more frequently than vortex nucleation (Bowley *et al.* 1982). Whether vortex nucleation and roton emission can be regarded as occurring independently is an important question, to which we shall return later.

(v) Even at velocities a little lower than the Landau critical velocity there is a complication associated with roton creation, as we see as follows.

If a sphere moves through an ideal incompressible fluid at speed U, then near the equator of the sphere the speed of the fluid relative to the sphere will exceed U; at the equator itself this relative speed is $\frac{3}{2}U$. Thus it is possible for the fluid speed near the equator of the sphere to

exceed the Landau critical velocity, even when the speed of the sphere as a whole does not. Under these conditions free roton creation is not possible, but there will be a tendency for localized (virtual) rotons to be formed, with a consequent modification to the velocity field round the ion. (If we use the ideas of Takken (1970), we see that there is some similarity here with the case of a sphere moving through a classical ideal compressible fluid at a Mach number between $\frac{2}{3}$ and 1, when a localized shock wave forms round the sphere; see also the ideas of Strayer *et al.* (1971)). This modification to the velocity field, together with that due to any distortion of the ion, will give rise to a dependence of ionic mass on velocity. However, recent measurements of Ellis *et al.* (1983) show that any modification to the effective mass is very small (less than 5 %), so that we are probably safe in assuming that the modification to the velocity field is not large. However, whether it is strictly negligible is unclear.

Our plan is as follows. We shall consider first the situation at zero temperature, when the moving ion can create vorticity only if the ion–liquid system does not thereby need to gain energy, and when the momentum (or, more accurately, the impulse) of the ion–liquid system must be conserved. Physically, it seems likely that the nucleation process will involve the formation of either a vortex ring encircling the ion, or a loop of vortex line out of the side of the ion. We shall therefore calculate (§3) the energy and impulse associated with an ion plus encircling vortex ring and with an ion plus vortex loop, as functions of the position and size of the ring or loop. We shall find that the minimum nucleation velocity is probably associated with the formation of a loop rather than a ring, and we shall evaluate this critical velocity. We shall also find that probably a small potential barrier impedes formation of the loop. In §4 we shall consider the possibility of quantum tunnelling through this barrier, and we shall suggest that such tunnelling might occur at a significant rate. In §5 we shall relax the condition that the temperature be zero, and we shall discuss the surmounting of the barrier by thermal activation. In §6 we compare our work with earlier theoretical work on these problems, and in §7 we compare with experiment.

As we shall see, our calculations indicate that vortex nucleation by a moving ion will always involve initially the formation of a vortex loop, as opposed to an encircling ring, except at ion velocities considerably in excess of the critical value for loop formation. At these high velocities the situation may change for two reasons. First, direct nucleation of an encircling ring may become possible, although, as we shall see, it seems very unlikely. Secondly, even if such direct nucleation does not occur, it might turn out that a vortex loop can evolve into an encircling ring. In either case, the resulting encircling ring might then become completely detached from the ion. Such behaviour could account for the recent unexpected experimental observation by Bowley *et al.* (1982) that at high pressure the apparent vortex nucleation rate falls off at high velocities and high electric fields. However, a proper treatment of the subsequent evolution of the nucleating vortex requires calculations of a type different from those reported in the present paper. These new calculations are now in progress, and we plan to publish the results in a later paper. In any case, the observation of Bowley *et al.* might be accounted for in a quite different way, as we shall explain in §7.

Strictly speaking, the energy and impulse of any configuration of vortex line depends on the structure of the core of the vortex, which is not known. It turns out that this is not a serious matter as long as the ratios $\tilde{R}/a_0$ and $\tilde{b}/a_0$ are reasonably large compared with unity, where a_0 is an effective vortex core radius, $\tilde{R}$ is the radius of curvature of the vortex loop or vortex ring, and $\tilde{b}$ is the spacing between the vortex and its image in the bounding surface of the ion. However,

PHILOSOPHICAL TRANSACTIONS OF THE ROYAL SOCIETY A MATHEMATICAL, PHYSICAL & ENGINEERING SCIENCES

when these inequalities are not satisfied there is considerable uncertainty in the energy and the impulse. Using the results of some model calculations of Jones & Roberts (1982), we shall make serious attempts to estimate the energy and impulse of the relevant vortex line configurations when $\tilde{R}/a_0$ or $\tilde{b}/a_0$ are small, but some uncertainty remains, which affects our estimates of both critical velocities and vortex nucleation rates. This uncertainty must persist until more is known about the vortex–core structure.

3. Calculations of critical velocities and energy barriers at $T = 0$

As we have explained, we shall assume that an ion moving through superfluid helium at zero temperature can be regarded as a rigid sphere, radius R_I and effective mass M_I, moving with velocity $\boldsymbol{U}$ through an ideal inviscid fluid of density ρ_s. We define the equatorial plane as a plane normal to the velocity $\boldsymbol{U}$ and passing through the centre of the sphere. We consider two configurations of quantized vortex that might be formed near the ion. The first is that considered by Schwarz & Jang (1973); i.e. a vortex ring encircling the ion in a plane parallel to the equatorial plane (figure 1*a*). The second is a circular vortex loop, attached to the sphere and meeting it normally, as shown in figure 1*b*; we confine our attention to loops with axes that intersect the line of axial symmetry of the original irrotational flow round the sphere. The sizes and positions of the configurations of vortex are specified by the coordinates (R_0, Z_0) and (R_0, θ_0) shown in figure 1*a*, *b*. We have computed the energy and impulse for both these types of ion–vortex complex, as functions of the coordinates (R_0, Z_0) or (R_0, θ_0) and of the speed U of the sphere, for values of R_I and M_I corresponding to the positive and negative ions at $T = 0$.

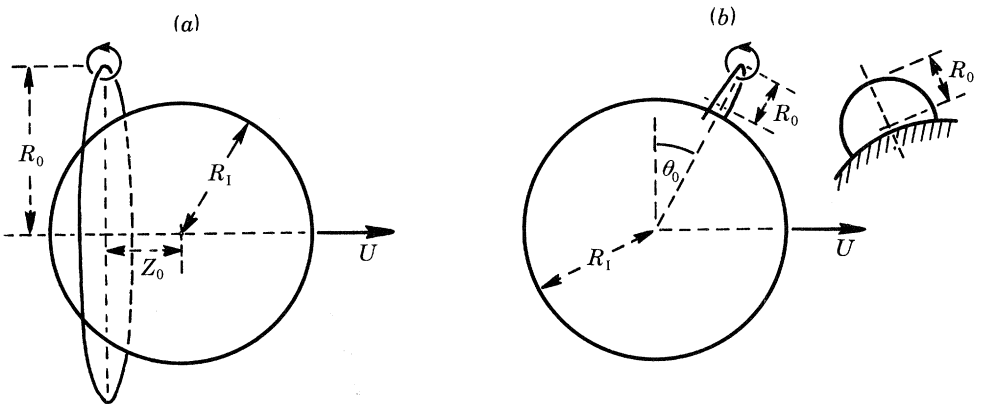

Figure 1. Geometry of the nucleating vortices: (*a*) the encircling ring; (*b*) the attached loop.

As explained by Schwarz & Jang (1973), the energy and impulse of ion–vortex complexes of this kind can be calculated from formulae that involve surface integrals of the velocity field and the associated vector potential over the surfaces of the sphere and of the vortex core, and we have used the same basic formulae in our own calculations. It is convenient to ensure that the boundary conditions at the surface of the sphere are satisfied by using the method of images. For the encircling rings shown in figure 1*a*, the necessary image is easily found and is simply a second ring inside the sphere. For the vortex loops (figure 1*b*) the necessary image is more complicated, and we shall devote §3.1 to a discussion of its form.

In the next three sections we shall base our calculations on methods that are accurate only if

the ratios $\tilde{R}/a_0$ and $\tilde{b}/a_0$, defined in §2, are large compared with unity (the 'thin core' approximation). The corrections necessary when these conditions are not satisfied form the subject of §3.4.

3.1. *The image of a vortex loop in a sphere*

It is helpful to consider this problem in terms of electromagnetic analogies. The velocity field corresponding to the flow of an ideal fluid induced in the neighbourhood of a sphere when a vortex loop is attached is analogous to the magnetic field induced in the neighbourhood of a superconducting sphere when a thin current loop is attached (the current through the loop passing also along the surface of the sphere, so that there is a complete circuit). We are therefore led to consider the image of a short current element, $i\,\mathrm{d}\boldsymbol{l}$, when it is placed outside a superconducting sphere. Suppose first that the current element points in a direction along a radius vector of the sphere (figure 2*a*), and let this radius vector be the z-axis of a system of cylindrical polar coordinates. The vector potential ($\boldsymbol{A}$) due to the current element alone will then have the form

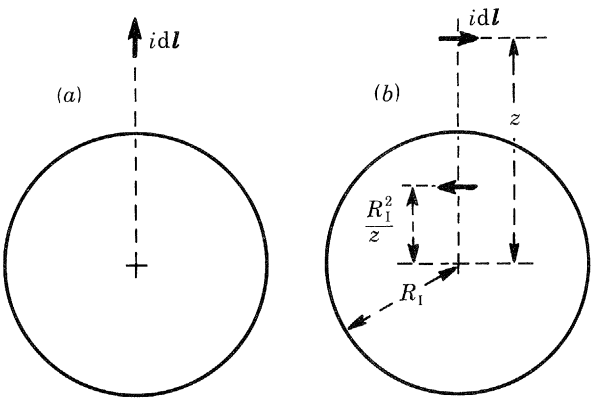

FIGURE 2. Images of current elements in a superconducting sphere.

$(0, 0, A_z(r, z))$, and the resulting magnetic field ($\boldsymbol{B}$) the form $(0, B_\phi(r, z), 0)$. (We choose the gauge of $\boldsymbol{A}$ so that $\operatorname{div}\boldsymbol{A} = 0$.) Since $\boldsymbol{B}$ must satisfy the condition that its normal component vanishes at the surface of the sphere, there is in this case no need for any image, although an image can be added, in the form of any current element lying at any point on, and in the direction of, the z-axis, without violating the boundary conditions. If the current element is perpendicular to the radius vector (figure 2*b*), the boundary condition can be satisfied if an image is added so that the total vector potential is zero over the surface of the sphere. If we remember that the vector potential due to a current element is given by a formula $\boldsymbol{A} = \mu_0 i\,\mathrm{d}\boldsymbol{l}/4\pi|r|$, analogous to that giving the electrostatic scalar potential due to a point charge, we see that the necessary image can be obtained by reference to the electrostatic analogue of a point charge outside a conducting sphere. The image current element is therefore at the position and direction given in figure 2*b*, and it has a magnitude $(R_1/z)\,i\,\mathrm{d}l$.

With the help of these preliminary results we can deduce the image of the vortex loop (figure 3). Consider the current element BA in this loop. The component of this element in the plane of the loop and at right angles to the line OA requires an image, which turns out from the geometry of the problem to be at the point C, where C is on the extension of the circle formed by the vortex loop. The component parallel to AO does not *require* an image, but we shall give it an image, at

the point C and directed along OA, in such a way that the total resultant image at C points along the circle through C. That this can be done suggests at first sight that the image of the current loop is simply the extension of the loop through the sphere. However, it is easily seen from our preliminary discussion that the magnitude of the image current-element is not equal to simply $i|\overrightarrow{CD}|$, where i is the current in the external part of the current loop; it is in fact equal to $(R_I/|\overrightarrow{OC}|)\, i|\overrightarrow{CD}|$. Thus, if the length of the image is to equal $|\overrightarrow{CD}|$, as we would like it to be, then current in the image loop is not conserved. We must therefore add extra image currents to achieve current conservation. If these extra currents are not to interfere with the boundary conditions on the surface of the sphere they must flow radially from or to the centre of the sphere. They must therefore form a kind of fan, the currents flowing from the points of the part FE of the circular image towards O and from O towards points on the part EG of the circular image.

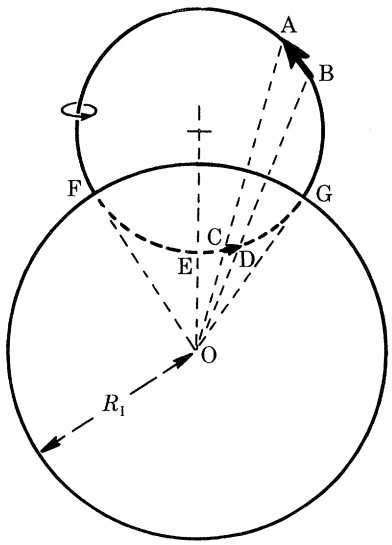

FIGURE 3. Image of a vortex loop in a solid sphere.

In summary, therefore, the image of the current loop FAG is the rest of the loop GEF, together with a distribution of radial currents flowing between the centre, O, of the sphere and points along the image GEF. The current at the point C in the image loop is equal to $R_I/|\overrightarrow{OC}|$ times the current in the real external loop, and the radial currents are adjusted to enforce current conservation. The obvious hydrodynamic analogue of this is the image that we require for our vortex loop (velocity field, $\boldsymbol{v} \equiv \boldsymbol{B}$; hydrodynamic circulation, $\kappa \equiv \mu_0 i$).

3.2. *Some useful simplifying formulae*

In this section we shall derive some results that serve to simplify the computations to be described in the next section.

Let $\boldsymbol{P}_0(U)$ and $E_0(U)$ be the impulse and energy associated with an ion moving in superfluid helium at zero temperature in the absence of vorticity, and let $\boldsymbol{P}_c(U)$ and $E_c(U)$ be the impulse and energy of an ion–vortex line complex, the ion moving with velocity U. (We shall say that $\boldsymbol{P}_0$ and E_0 refer to the free ion.) Then we find that these relations hold:

$$\boldsymbol{P}_c(U) = \boldsymbol{P}_c(0) + \boldsymbol{P}_0(U), \quad E_c(U) = E_c(0) + E_0(U). \qquad (3.2.1), (3.2.2)$$

The first of the relations must obviously be correct because the impulse depends linearly on fluid velocity and is therefore additive. The second relation requires proof as follows.

Let $\boldsymbol{v}_1$ be the velocity field in the superfluid due to the vortex and its image, for a stationary ion, and let $\boldsymbol{v}_2$ be the (dipole) velocity field due to motion of the ion. The latter velocity field is irrotational, and therefore we can write $\boldsymbol{v}_2 = \nabla\phi$, where ϕ is a scalar field. The kinetic energy associated with the flow $\boldsymbol{v}_1 + \boldsymbol{v}_2$ is given by

$$T_F = \tfrac{1}{2}\rho_s \int (\boldsymbol{v}_1 + \boldsymbol{v}_2)^2 \,\mathrm{d}\tau = \tfrac{1}{2}\rho_s \int \boldsymbol{v}_1^2 \,\mathrm{d}\tau + \tfrac{1}{2}\rho_s \int \boldsymbol{v}_2^2 \,\mathrm{d}\tau + \rho_s \int \boldsymbol{v}_1 \cdot \boldsymbol{v}_2 \,\mathrm{d}\tau. \tag{3.2.3}$$

The last term on the right side of this expression can be written

$$\int (\boldsymbol{v}_1 \cdot \boldsymbol{v}_2)\,\mathrm{d}\tau = \int \mathrm{div}\,(\phi \boldsymbol{v}_1)\,\mathrm{d}\tau - \int \phi\,\mathrm{div}\,\boldsymbol{v}_1\,\mathrm{d}\tau = \int \phi \boldsymbol{v}_1 \cdot \mathrm{d}\boldsymbol{S} - \int \phi\,\mathrm{div}\,\boldsymbol{v}_1\,\mathrm{d}\tau. \tag{3.2.4}$$

The surface integral is over the surface of the ion and over a surface at infinity, and it must therefore vanish. To a good approximation flow of the superfluid is incompressible, and therefore the last term in (3.2.4) also vanishes. Therefore the last term in (3.2.3) vanishes, and the result (3.2.2) follows immediately.

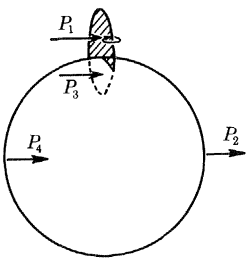

FIGURE 4. To illustrate the impulse associated with a vortex loop attached to a solid sphere.

The second useful result is that the impulse $\boldsymbol{P}_c(0)$ is equal simply to the impulse associated with the vortex line outside the ion together with its image inside the ion, the vortex line and its image being regarded as situated in the unbounded fluid. The proof is now given.

The ion–vortex line complex is shown schematically in figure 4. Since we are interested in the value of $\boldsymbol{P}_c(0)$, the ion remains at rest when the vortex is created. It was proved by Schwarz & Jang (1973) that $\boldsymbol{P}_c(0)$ can be written in the form

$$\boldsymbol{P}_c(0) = \boldsymbol{P}_1 + \boldsymbol{P}_2, \tag{3.2.5}$$

where

$$\boldsymbol{P}_1 = \tfrac{1}{2}\rho_s \int (\boldsymbol{r} \times \boldsymbol{\omega})\,\mathrm{d}\tau \tag{3.2.6}$$

and

$$\boldsymbol{P}_2 = \tfrac{1}{2}\rho_s \int \boldsymbol{r} \times (\mathrm{d}\boldsymbol{S} \times \boldsymbol{v}), \tag{3.2.7}$$

the volume integral being taken over the whole volume of superfluid, and the surface integral over the surface of the ion. The vorticity in the superfluid is $\boldsymbol{\omega}$, and therefore the integral (3.2.6) can be replaced by the integral

$$\boldsymbol{P}_1 = \tfrac{1}{2}\rho_s \kappa \int \boldsymbol{r} \times \mathrm{d}\boldsymbol{l} \tag{3.2.8}$$

along the core of the vortex line. The way in which $\boldsymbol{P}_c(0)$ can be split into two components $\boldsymbol{P}_1$ and $\boldsymbol{P}_2$ is not uniquely defined since these latter integrals depend on the origin of coordinates.

However, we shall choose this origin in such a way that $\boldsymbol{P}_1$ has a value equal to $\rho_s\kappa$ times the area bounded by the vortex and the surface of the ion (the area shown shaded in figure 4); $\boldsymbol{P}_1$ can then be interpreted as the total impulse arising from an impulsive pressure $\rho_s\kappa$ applied to this area, and $\boldsymbol{P}_2$ will be the total impulse arising from a suitable impulsive pressure applied to the fluid at the surface of the ion.

Now suppose that the ion is removed and that we create in the unbounded fluid a vortex system consisting of the original vortex together with its image in the ion. The required impulse will be equal to $\boldsymbol{P}_1+\boldsymbol{P}_3$, where $\boldsymbol{P}_3$ is obtained from an expression of the form (3.2.8) evaluated for the image system of vortices. Let us now imagine that we divide the fluid into two volumes: the volume inside a sphere placed in the position originally occupied by the ion; and the volume outside this sphere. The impulse acting on the inner volume will be the sum of $\boldsymbol{P}_3$ and an impulse $\boldsymbol{P}_4$ acting at the spherical boundary of this inner volume, this last impulse arising from an impulsive pressure derived from the fluid outside the inner volume. The impulse on the outer volume will be the sum of $\boldsymbol{P}_1$ and an impulse $\boldsymbol{P}_2$ acting outwards through the spherical hole formed by the inner volume. The impulses $\boldsymbol{P}_2$ and $\boldsymbol{P}_4$ must clearly balance, so that $\boldsymbol{P}_2+\boldsymbol{P}_4=0$. Now the fluid inside the inner volume acquires no net momentum as a result of the application of the impulses $\boldsymbol{P}_3$ and $\boldsymbol{P}_4$, since the image vortex is such that there is no fluid flow through the boundary of this volume. It follows that $\boldsymbol{P}_3+\boldsymbol{P}_4=0$, and therefore that

$$\boldsymbol{P}_1+\boldsymbol{P}_2=\boldsymbol{P}_1+\boldsymbol{P}_3, \tag{3.2.9}$$

which is the result that we wish to prove.

3.3. *Computational techniques*

Our computations are based on formulae that are the same as those used by Schwarz & Jang (1973). We express the superfluid velocity field $\boldsymbol{v}$ in terms of a vector potential $\boldsymbol{A}$ ($\boldsymbol{v}=\operatorname{curl}\boldsymbol{A}$). The total kinetic energy associated with an ion–vortex line complex can then be written

$$E_c(U)=\tfrac{1}{2}M_{I0}U^2+\tfrac{1}{2}\rho_s\int v^2\mathrm{d}\tau=\tfrac{1}{2}M_{I0}U^2-\tfrac{1}{2}\rho_s\int(\boldsymbol{A}\times\boldsymbol{v})\cdot\mathrm{d}\boldsymbol{S}, \tag{3.3.1}$$

where M_{I0} is the mass of the bare ionic structure when removed from the fluid (i.e. for the positive ion M_{I0} is the mass of solid helium formed by electrostriction; for the negative ion M_{I0} is practically zero), and the surface integral is taken over the surfaces of both the ion and the core of the vortex line. For the special case of the free ion (no vortex line), equation (3.3.1) can be evaluated analytically, $\boldsymbol{v}$ being then simply a dipole field, and we obtain the familiar result

$$E_0(U)=\tfrac{1}{2}M_I U^2, \tag{3.3.2}$$

where

$$M_I=M_{I0}+\tfrac{2}{3}\pi\rho_s R_I^3. \tag{3.3.3}$$

When vortex line is present we then make use of the 'thin core' approximation, to which we have already referred. This approximation affects the contribution from the vortex core to the surface integral in (3.3.1). In evaluating this contribution we must insert in the integrand of this surface integral contributions from the velocity fields due to the dipole flow round the ion, the image vortex and the vortex itself. In the thin core approximation we replace the first two of these velocity fields by their values at the centre of the core, and in evaluating the effect of the third we make use of the approximation that leads to the asymptotic formula

$$E=\tfrac{1}{2}\rho_s\kappa^2 R\{\ln(8R/a_0)-1.62\} \tag{3.3.4}$$

for the kinetic energy associated with a vortex ring of radius R in an unbounded fluid (Lamb (1952), p. 236; but for the origin of the term 1.62 in his paper, see §3.4 in this one).

For the case when a vortex ring encircles the ion, considered by Schwarz & Jang (1973), these approximations lead to an evaluation of $E_c(U)$ in analytical terms. When $U = 0$ the total vector potential due to the vortex ring and its image can be chosen so that it vanishes at the surface of the sphere, and therefore $E_c(0)$ reduces to an integral over only the core of the vortex. This integral splits into two parts: that associated with the fluid velocity and vector potential due to the encircling vortex itself; and that associated with the vector potential at the core of the encircling vortex due to the image. The first part leads to a contribution to $E_c(0)$ of the form (3.3.4) for the encircling ring; the second part leads to an expression that can be evaluated in terms of elliptic integrals (see Schwarz & Jang 1973). This procedure leads to an evaluation of $E_c(0)$, from which $E_c(U)$ can be obtained with the help of (3.2.2).

For vortex loops, the vector potential at the surface of the sphere cannot vanish even when $U = 0$, so that contributions to $E_c(0)$ arise from integrals over both the surface of the sphere and the surface of the vortex core. Both integrals need to be evaluated numerically. The former integral is evaluated by summing over a finite number (of order 1000) of surface elements, smaller elements being used in regions where the velocity field or vector potential are changing rapidly with position on the sphere. The latter integral is evaluated by first taking the integral for the complete isolated vortex ring, which yields the analytical expression (3.3.4), and then making corrections for the following two modifications. First, a fraction of the ring is missing, and the integral is correspondingly reduced. Secondly, the vector potential and velocity field at the surface of the core of the vortex are changed because the missing part of the complete ring is replaced by the image system described in §3.1. Evaluation of this second correction is made by replacing the vortex loop and its image by a finite number (of order 500) of straight sections and then making an appropriate summation. These procedures again lead to an evaluation of $E_c(0)$, from which $E_c(U)$ is obtained with the help of (3.2.2).

So far in this section we have considered only the calculation of the energy. Calculation of the impulse is based on (3.2.6) together with (3.2.1) and the fact (proved in §3.2) that the impulse $\boldsymbol{P}_c(0)$ is equal simply to the impulse associated with the vortex line outside the ion together with its image inside the ion, the vortex line and its image being regarded as existing in the unbounded fluid. Again the thin core approximation is used, so that in evaluating (3.2.6) it is assumed that the vorticity $\boldsymbol{\omega}$ is concentrated along a line at the centre of the vortex core. For a vortex ring encircling the ion we are led to an evaluation of $\boldsymbol{P}_c(U)$ in analytic terms, as with the energy. For vortex loops numerical integration is required, which we have again done by replacing the vortex loop and its image by a finite number of straight sections and then making the appropriate summation.

Later in this paper, and more particularly in later papers, we shall be interested in the velocity with which elements of the vortex line move relative to the ion. Now we know that any element of vortex line moves with the local fluid velocity, this local velocity being due to the rest of the vortex line and its image and to the dipole field associated with the moving ion. The velocity field due to the rest of the vortex line and its image can be evaluated from the equation

$$\boldsymbol{v}(\boldsymbol{r}) = \frac{1}{4\pi}\int \frac{\boldsymbol{\omega}(\boldsymbol{r}') \times (\boldsymbol{r} - \boldsymbol{r}')}{|\boldsymbol{r} - \boldsymbol{r}'|^3}\, \mathrm{d}^3\boldsymbol{r}', \tag{3.3.5}$$

which gives the velocity field at point $\boldsymbol{r}$ due to the distribution of vorticity $\boldsymbol{\omega}(\boldsymbol{r}')$. In evaluating

(3.3.5) we again use a thin core approximation, as we did in connexion with the calculation of the energy. For the encircling ring, the contribution (3.3.5) at a point on the ring splits into two parts, that due to the rest of the ring itself, and that due to the image. The former contribution gives rise simply to a uniform translation of the ring in the z-direction (figure 1*a*) at a rate given by the well known equation

$$u_z = (\kappa/4\pi R_0)\{\ln(8R_0/a_0) - 0.62\}, \tag{3.3.6}$$

where R_0 is the radius of the ring. The latter contribution causes each element of the ring to move in both the z- and the r-directions, with velocities given by

$$u_Z = \frac{\lambda^{\frac{1}{2}}\kappa R_0}{4\pi}\int_0^{2\pi} \frac{(\lambda R_0 - R_0\cos\theta)\,\mathrm{d}\theta}{\{\lambda^2 R_0^2 + R_0^2 - 2\lambda R_0^2\cos\theta + (Z_0 - \lambda Z_0)^2\}^{\frac{3}{2}}}, \tag{3.3.7}$$

$$u_r = -\frac{\lambda^{\frac{1}{2}}\kappa R_0}{4\pi}\int_0^{2\pi} \frac{(Z_0 - \lambda Z_0)\cos\theta\,\mathrm{d}\theta}{\{\lambda^2 R_0^2 + R_0^2 - 2\lambda R_0^2\cos\theta + (Z_0 - \lambda Z_0)^2\}^{\frac{3}{2}}}, \tag{3.3.8}$$

where $\lambda = R_1^2/(R_0^2 + Z_0^2)$. For vortex loops we have evaluated the contribution (3.3.5) at any point on the loop by a method similar to the one we used for the energy; i.e. we first evaluate the velocity for the complete isolated ring, which yields an equation similar to (3.3.6), and then make corrections because part of the ring is missing and is replaced by an image. These corrections require numerical integration.

We have made careful checks on the accuracy of our numerical integrations by varying the number of finite elements into which the vortex lines, their images and the ion surface are split and by making comparisons with analytical results in appropriate limiting cases. We believe that our results for both the energy and impulse are accurate to about $\pm 0.5\%$.

3.4. *Corrections required when the vortex core is close to the surface of the ion*

As we have already explained, the methods described in §3.3 will yield reasonably accurate results only if the ratios $\tilde{R}/a_0$ and $\tilde{b}/a_0$ are large compared with unity; i.e. if the vortex loops have radii large compared with a_0 and if the cores of the encircling vortex rings are separated from the ion surface by a distance large compared with a_0. In this section we discuss the corrections that are necessary when these conditions are not satisfied.

We must emphasize first that these corrections could be calculated accurately only if we were in possession of detailed and realistic theories of both the structure of the vortex core and of the conditions near the solid–helium II boundary. Such theories do not exist, and we must therefore rely on theories that are more or less unrealistic. Even then the calculations would be very difficult, since they must involve not only the vortex core itself but also its interaction with a solid boundary, in situations that often lack any simplifying symmetry. We shall therefore make what we believe are reasonable guesses based on the simplest assumption about the liquid–solid boundary and on the results of the calculations of other authors that are strictly relevant only to vortex rings or vortex pairs in an unbounded fluid.

Consider first the energy and impulse associated with a vortex ring, radius R, in an unbounded fluid, where R is comparable with the core radius a_0. Calculations for rings in a classical fluid have been published by Norbury (1973). Calculations based on solutions of the Ginsburg–Pitaevskii equation, and therefore of possible relevance to a quantum fluid, have been published by Jones & Roberts (1982) (earlier calculations of a similar type by Blood (1976) gave results rather different to those of Jones & Roberts, but they seem to have been based on unjustified

approximations). In both cases the calculations relate to disturbances that (*a*) preserve their form as they propagate through the fluid and (*b*) have a form corresponding to an ordinary vortex ring in the limit as R/a_0 becomes large compared with unity. We shall assume in due course that the evolution of one of these disturbances from a small to a large value of R/a_0 can be taken to represent the route by which a vortex ring is formed from the vortex-free fluid.

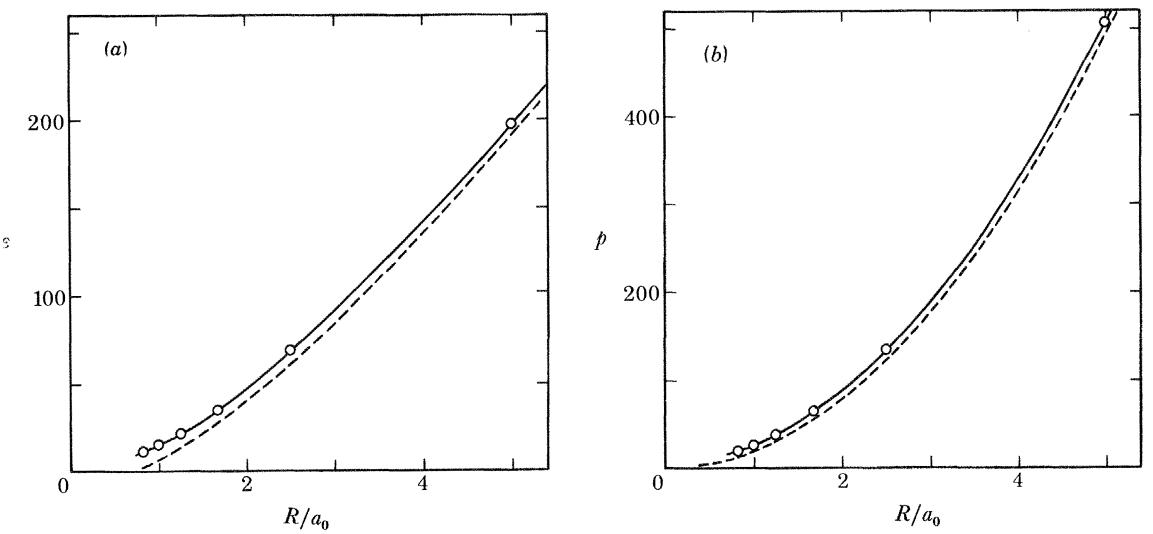

FIGURE 5. Plots of (*a*) ϵ and ϵ_0, and (*b*) p and p_0, against R/a_0, for the classical vortex rings of Norbury (1973); where ϵ and ϵ_0 are energies in units of $\rho\kappa^2 a_0/4\pi^2$; p and p_0 are impulses in units of $\rho\kappa a_0^2/2\pi$.

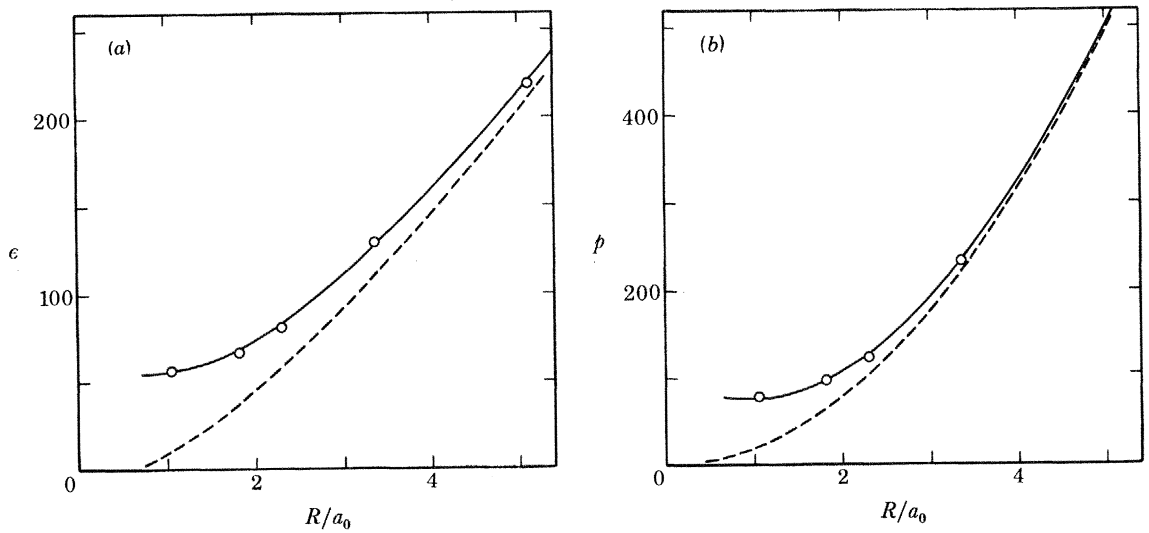

FIGURE 6. Plots of (*a*) ϵ and ϵ_0, and (*b*) p and p_0, against R/a_0 for the quantum vortex rings of Jones & Roberts (1982).

The results of the calculations of Norbury (1973) and of Jones & Roberts (1982) are shown by points in figures 5 and 6, respectively. The points have been joined by our own smooth curves. The results exist only for a limited number of values of R/a_0 because the calculations have to be made numerically. The broken lines in figures 5 and 6 are plots of either

$$\epsilon_0 = 2\pi^2 R\{\ln(8R/a_0) - 2 + \delta\}/a_0 \quad \text{or} \quad p_0 = 2\pi^2 R^2/a_0^2, \qquad (3.4.1), (3.4.2)$$

where $\delta = 0.25$ for the classical (Norbury) rings and $\delta = 0.38$ for the quantum (Jones–Roberts) rings. The quantities ϵ_0 and p_0 are the energy and impulse (in dimensionless units) expressed in the usual form that is asymptotically correct only in the limit of large R/a_0; they are therefore equivalent to the uncorrected values of energy and impulse with which we were concerned in the last section. For the classical rings our solid lines are merely a guide to the eye, but for the quantum rings they are given by the analytical expressions

$$\epsilon = \epsilon_0 + 55\epsilon_0\{\epsilon_0(1 + \tfrac{1}{50}\epsilon_0)\}^{-1} \tag{3.4.3}$$

and

$$p = p_0 + 85p_0\{p_0(1 + \tfrac{1}{40}p_0)\}^{-1}. \tag{3.4.4}$$

These expressions have been introduced for convenience of calculation; they have no theoretical foundation. It should be noted that our plots do not extend to values of R/a_0 much less than unity, for the obvious reason that R and a_0 then cease to have significance. Indeed, for the quantum rings, Jones & Roberts (1982) found that disturbances that preserve their form and tend to become vortex rings for large R/a_0 do not exist for values of ϵ and p less than 50.7 and 69.6 respectively. At this point the 'vortex ring' has ceased to have associated with it any vorticity, and it becomes indistinguishable from a rarefaction sound pulse. (In fact, for ϵ and p having values in excess of the critical values 50.7 and 69.6 the ϵ against p curves have two branches that meet in a cusp at the critical values; the lower branch is the vortex ring, with which we are concerned, and the upper branch is a sound pulse.) However, as we shall see, the precise behaviour of a 'vortex ring' when R/a_0 is significantly less than unity is probably not of great importance to us, although strictly speaking we have not explicitly identified a *complete* path along which a vortex ring can be formed from the undisturbed state.

Figures 5 and 6 confirm that corrections to the energy and impulse of a vortex ring when R/a_0 is not large do indeed depend substantially on the details of the core structure. The classical vortex rings have cores that are filled with liquid having a vorticity proportional to the distance from the axis of symmetry of the ring. In this case the corrections are quite small, except when the ring has collapsed to such an extent that it is no longer a real ring. The quantum rings have cores in which there is no vorticity but in which the fluid density falls to zero at the core centre. In this case the corrections are substantial. The different behaviour in the two cases must arise from one or both of two essential differences in the core structure: the core of the quantum vortex is essentially hollow, while that of the classical vortex has uniform density; and the energy of the quantum vortex contains a contribution from the curvature in the amplitude of the condensate wave function, which is absent in the classical case. It is unlikely that either type of vortex is a realistic model for a vortex in superfluid helium. The quantum vortex is likely to be the better, because it includes the effect of the curvature in the amplitude of the condensate wavefunction, but it may lead to overestimated corrections because the core of a vortex in helium may not be hollow (Fetter 1971). Indeed, there is experimental evidence that some types of normal fluid or excitations are associated with the core (Glaberson 1969). We shall in fact make use of the results for the quantum vortex ring, as we now explain.

The results of figures 5 and 6 refer to complete rings existing in an unbounded field. Suppose that the fluid is now bounded by a solid infinite flat plane, and that attached to this plane is a semicircular vortex loop. We shall assume that at the solid boundary the effective density of the fluid (the superfluid density) is a simple step function; i.e. that there is no 'healing' at the surface of the solid. In this case the energy and impulse of the vortex loop must be just one half those for

the complete vortex ring in an infinite fluid. For a quantum semicircular loop, therefore, we can obtain the energy and impulse by first calculating values for the asymptotic limit (large R/a_0) and then multiplying by factors derived from the right sides of (3.4.3) and (3.4.4). We have adopted a similar procedure with a vortex loop attached to an ion. For the energy, we have added to the results obtained by the methods of §3.3, a quantity equal to the product of the energy of the complete ring, the fraction of the ring that is not missing and the term in square brackets on the right side of (3.4.3). For the impulse, we have added a quantity equal to the product of the impulse of the complete ring, the fraction of ring that is not missing and the term in square brackets on the right side of (3.4.4). Of course this procedure is unlikely to be strictly correct, but we guess that it will not introduce errors more significant than those already inherent in the use of the model calculations of Jones & Roberts (1982). We guess that the results will be qualitatively correct, but are likely to be quantitatively in error. The extent of the probable error is impossible to judge in the absence of realistic models of the vortex core and of the solid–liquid boundary. Fortunately, as we shall see, our final results turn out to be not very sensitive to the precise magnitude of the corrections discussed in the present section.

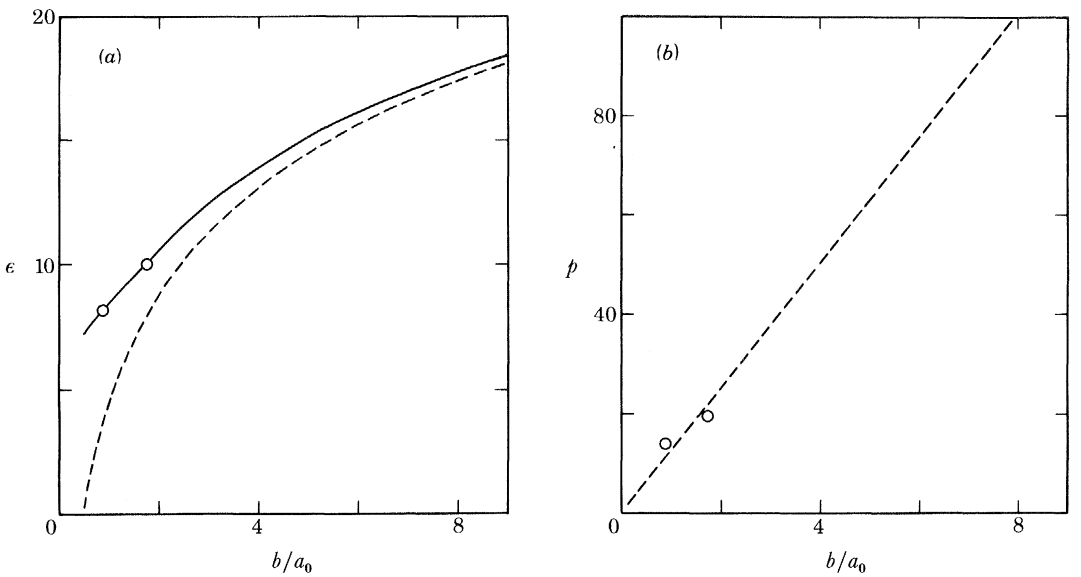

FIGURE 7. Plots of (*a*) ϵ and ϵ_0, and (*b*) p and p_0, against b/a_0 for the quantum vortex pairs of Jones & Roberts (1982); where ϵ and ϵ_0 are energies per unit length in units of $\rho\kappa^2/4\pi^2$; p and p_0 are impulses per unit length in units of $\rho\kappa a_0/2\pi$.

To deal with the vortex ring that encircles the ion (the Schwarz–Jang case) we consider first a pair of infinitely long parallel rectilinear vortices with equal and opposite strengths. In the limit as the separation, $2b$, becomes large compared with the core radius a_0, the energy and impulse per unit length of such a pair are given in dimensionless units by

$$\epsilon_0 = 2\pi \ln (2b/a_0) \quad \text{and} \quad p_0 = 4\pi b/a_0; \qquad (3.4.5), (3.4.6)$$

these quantities are plotted as functions of b/a_0 in figure 7. As far as we know, there exist no calculations for a classical vortex pair with small b/a_0, analogous to those of Norbury (1973) for the vortex ring. However, calculations for the quantum vortex pair were included in the paper by Jones & Roberts (1982), and the results are shown by the points in figure 7. Unfortunately, the

calculations included only two values of b/a_0 that are large enough for b and a_0 to remain meaningful; i.e. for vortex pairs that have not collapsed to such an extent that they cease to be identifiable as vortex pairs. The corrections to (3.4.5) and (3.4.6) are therefore very uncertain. For the impulse, we judge that no significant correction is required. For the energy, we have very tentatively represented the correction by the solid line in figure 7*a*, where the line has the analytical form

$$\epsilon = \epsilon_0 + 7.2\epsilon_0[\epsilon_0\{1 + 1.88(b/a_0 - 0.5)^{1.15}\}]^{-1}; \tag{3.4.7}$$

again this form has no theoretical foundation.

Now suppose that we have a single rectilinear vortex running parallel to an infinite plane solid surface. Using again the assumption of no healing at the solid–liquid boundary, we see that the energy and impulse associated with this line will be just one half that associated with the vortex pair. This situation is clearly similar to that obtained with the encircling vortex ring, provided that the spacing between the ring and ion (equivalent to b) is small compared with both the ionic radius and the radius of the ring. Therefore, for an encircling vortex ring that is sufficiently close to the ion and not too far from the equatorial plane, it seems appropriate to make a correction to the energy that is based on (3.4.7), where b is taken to be the minimum separation between the centre of the core of the ring and the surface of the ion. However, for the more general encircling vortex ring this procedure is not appropriate; for example, for a small ring far from the ion a correction based on (3.4.3) would obviously be more appropriate. We have therefore aimed for a form of correction that will interpolate smoothly between these two extreme cases. It turns out that this can be achieved as follows. For the impulse, we have simply applied to all rings a correction based on (3.4.4) for the complete ring. For the energy, we have first calculated a correction C_{R} from equation (3.4.3) and a correction C_{L} from (3.4.7); we have then based our correction to the energy on a correction C derived from C_{R} and C_{L} by means of the formula

$$C = C_{\mathrm{R}}\left(\frac{C_{\mathrm{R}}}{C_{\mathrm{R}} + C_{\mathrm{L}}}\right) + C_{\mathrm{L}}\left(\frac{C_{\mathrm{L}}}{C_{\mathrm{R}} + C_{\mathrm{L}}}\right). \tag{3.4.8}$$

As for the vortex loop this procedure is, we hope, qualitatively correct, but quantitatively it must be in error by an amount that is at present impossible to estimate. Again, however, our final results turn our not to be very sensitive to the precise magnitude of the correction.

3.5. *Results of the computations*

The results of the calculations described in the preceding sections are summarized in figures 8–13. We denote by U the initial speed of the free ion; by $\Delta E_{\mathrm{R}}(U, R_0, Z_0)$ the change in energy, at constant impulse, when an encircling vortex ring is formed with the geometry of figure 1*a*; and by $\Delta E_{\mathrm{L}}(U, R_0, \theta_0)$ the change in energy, at constant impulse, when a vortex loop is formed with the geometry of figure 1*b*. Figure 8*a–d* refers to the formation of vortex loops in the equatorial plane and contains plots of $\Delta E_{\mathrm{L}}(U, R_0, 0)$ against R_0 for positive and negative ions, various pressures, and various values of U. Figure 9*a–d* shows the corresponding figures for encircling vortex rings in the equatorial plane. Figure 10*a–d* refers again to vortex loops and shows how $\Delta E_{\mathrm{L}}(U, R_0, \theta_0)$ behaves when the loops are out of the equatorial plane. Figure 11*a–g* shows the corresponding figures for encircling vortex rings. Our computations are based on values of the ionic radii and masses given by Schwarz & Jang (1973) and on the following values of the core

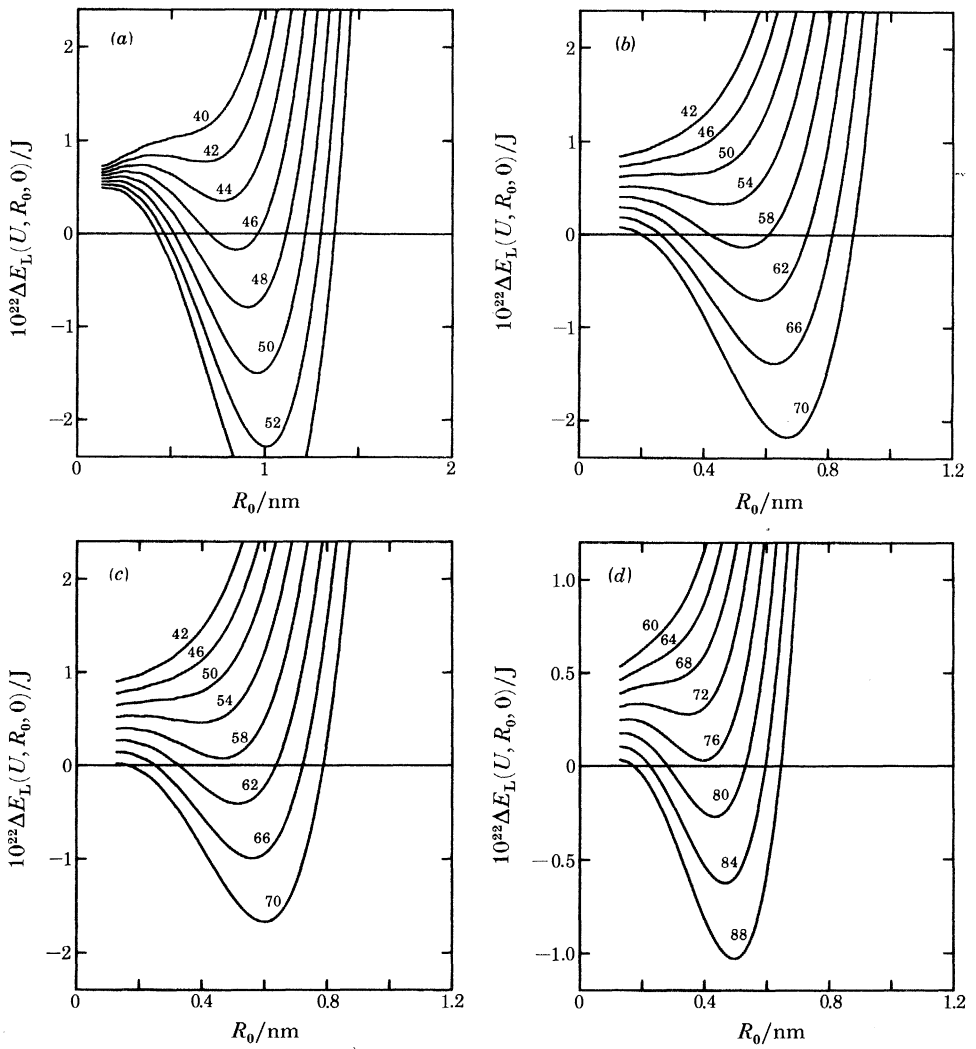

FIGURE 8. $\Delta E_L(U, R_0, 0)$ plotted against R_0 for vortex loops in the equatorial plane for various initial ion velocities U. The figure against each curve is the value of U in metres per second: (*a*) negative ions, pressure 0 Pa; (*b*) negative ions, pressure 1.75×10^6 Pa; (*c*) negative ions, pressure 2.5×10^6 Pa; (*d*) positive ions, pressure 0 Pa.

parameter a_0, which we obtained from Steingart & Glaberson (1972): $P = 0$ Pa, $a_0 = 0.125$ nm; $P = 10^6$ Pa, $a_0 = 0.144$ nm; $P = 17.5 \times 10^5$ Pa, $a_0 = 0.152$ nm; $P = 2.5 \times 10^6$ Pa, $a_0 = 0.159$ nm. Values of the total density have been taken from Brooks & Donnelly (1977).

As we explained in §2, an ion–vortex complex can be formed at $T = 0$ only if $\Delta E = 0$. We define U_c as the minimum ion–velocity at which an ion–vortex complex can be so formed. Confining our attention first to vortex loops, we see that the most favourable (minimum energy) position for the loop is always in the equatorial plane. Corresponding values of U_c are shown in figure 12. At velocities higher than U_c vortex loops can be formed outside the equatorial plane. Our calculations confirm that the formation of an ion–vortex loop complex at velocities greater than U_c requires that a potential barrier be overcome. The barrier has a typical width of 4×10^{-10} m, and a typical height of probably 5×10^{-23} J. This estimate of the height is based on the assumption that the curves of $\Delta E_L(U, R_0, 0)$ do not rise in the region $R < 10^{-10}$ m; i.e. where

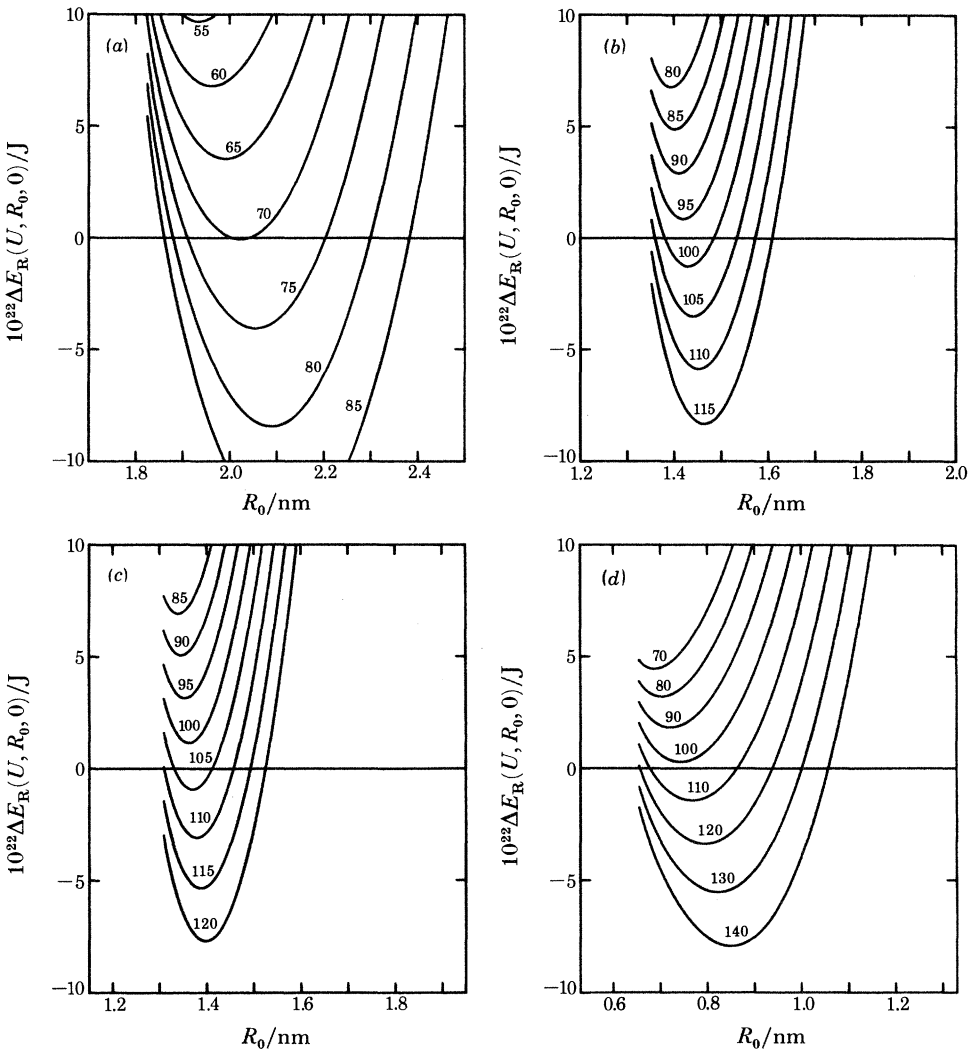

FIGURE 9. $\Delta E_R\,(U, R_0, 0)$ plotted against R_0 for encircling vortex rings in the equatorial plane for various initial ion velocities U. The figure against each curve is the value of U in metres per second: (*a*) negative ions, pressure 0 Pa; (*b*) negative ions, pressure 1.75×10^6 Pa; (*c*) negative ions, pressure 2.5×10^6 Pa; (*d*) positive ions, pressure 0 Pa.

R_0 has become significantly less than the vortex core diameter. This assumption seems reasonable in view of the fact that $\Delta E_L(U, R_0, 0)$ must fall toward zero as the vortex loop disappears altogether.

The situation is more complicated for encircling vortex rings. Figure 9 shows that the critical velocity, U_c, for formation of a ring in the equatorial plane is much larger than that for a loop. However, figure 11 shows that a ring formed in the equatorial plane is at a saddle point in the energy surface, not at a minimum. In principle, therefore, rings can be formed away from the equatorial plane at lower velocities. However, as we see from figure 11, a ring formed at a velocity comparable with the critical velocity for a loop would be at a large distance from the ion and would be separated from it by a very large potential barrier. We believe therefore that such a ring would not be formed in practice, except possibly at ion velocities very much greater than those plotted in figure 12.

We have referred to our calculated energy surfaces as indicating the existence of *potential*

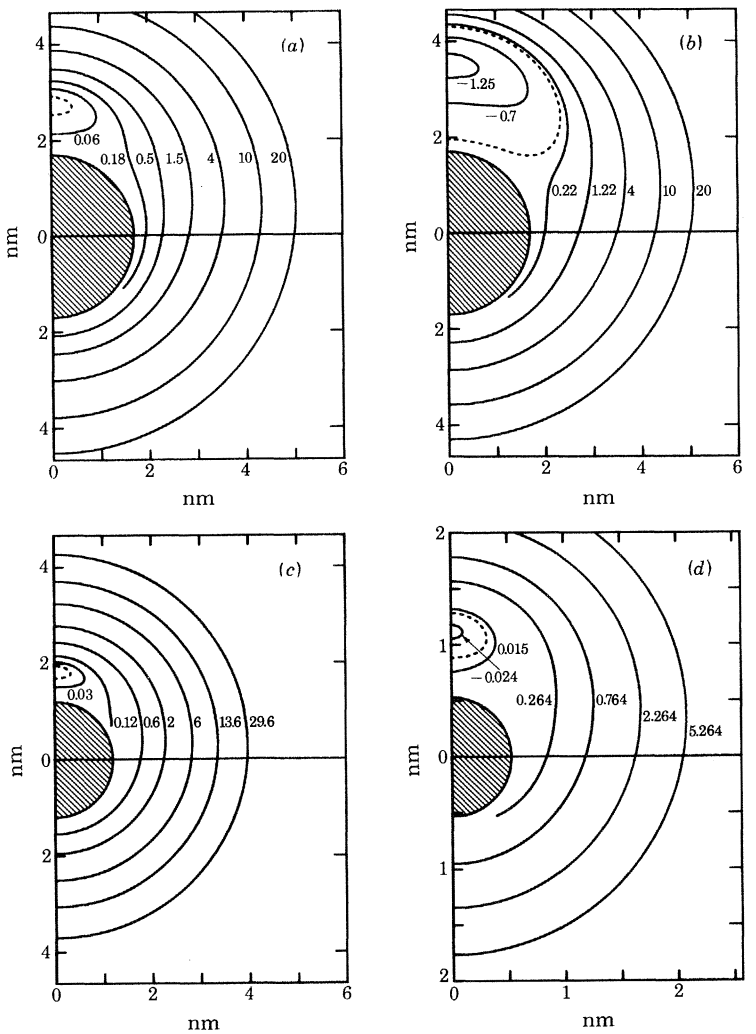

FIGURE 10. Contours of constant ΔE_L for vortex loops. Each graph is plotted on the plane of symmetry through the centre of the ion and parallel to the initial ion-velocity U. The size and position of a vortex loop is specified by the point at which the loop crosses this plane. The axes represent distances from the centre of the ion. The figure against each curve is the value of $10^{21}\,\Delta E_L/\mathrm{J}$. The broken curve is the contour $\Delta E_L = 0$; (*a*) negative ions, pressure 0 Pa, $U = 46\ \mathrm{m\,s^{-1}}$, $U_c = 45.5\ \mathrm{m\,s^{-1}}$; (*b*) negative ions, pressure 0 Pa, $U = 71\ \mathrm{m\,s^{-1}}$, $U_c = 45.5\ \mathrm{m\,s^{-1}}$; (*c*) negative ions, pressure 1.75×10^6 Pa, $U = 58\ \mathrm{m\,s^{-1}}$, $U_c = 57\ \mathrm{m\,s^{-1}}$; (*d*) positive ions, pressure 0 Pa, $U = 80\ \mathrm{m\,s^{-1}}$, $U_c = 76.5\ \mathrm{m\,s^{-1}}$.

barriers that tend to inhibit nucleation, in spite of the fact that a major contribution to the energy comes from the *kinetic* energy of flow. We shall aim to justify this description of the situation in the next section.

As we have already emphasized, the corrections described in §3.4 are based on a somewhat unrealistic theory and are unlikely to be quantitatively correct. It is therefore important to know whether the results described in the present section are very sensitive to the precise magnitude of these corrections. In figure 13 we show the effect of halving the correction factors, of correcting only the energy, and of applying no correction at all. We see that the corrections do have an important effect, especially for encircling rings, for which they produce results qualitatively different from those of Schwarz & Jang (1973) (it turns out, for example, that the latter results yield a minimum in the energy for rings in the equatorial plane, instead of a saddle point).

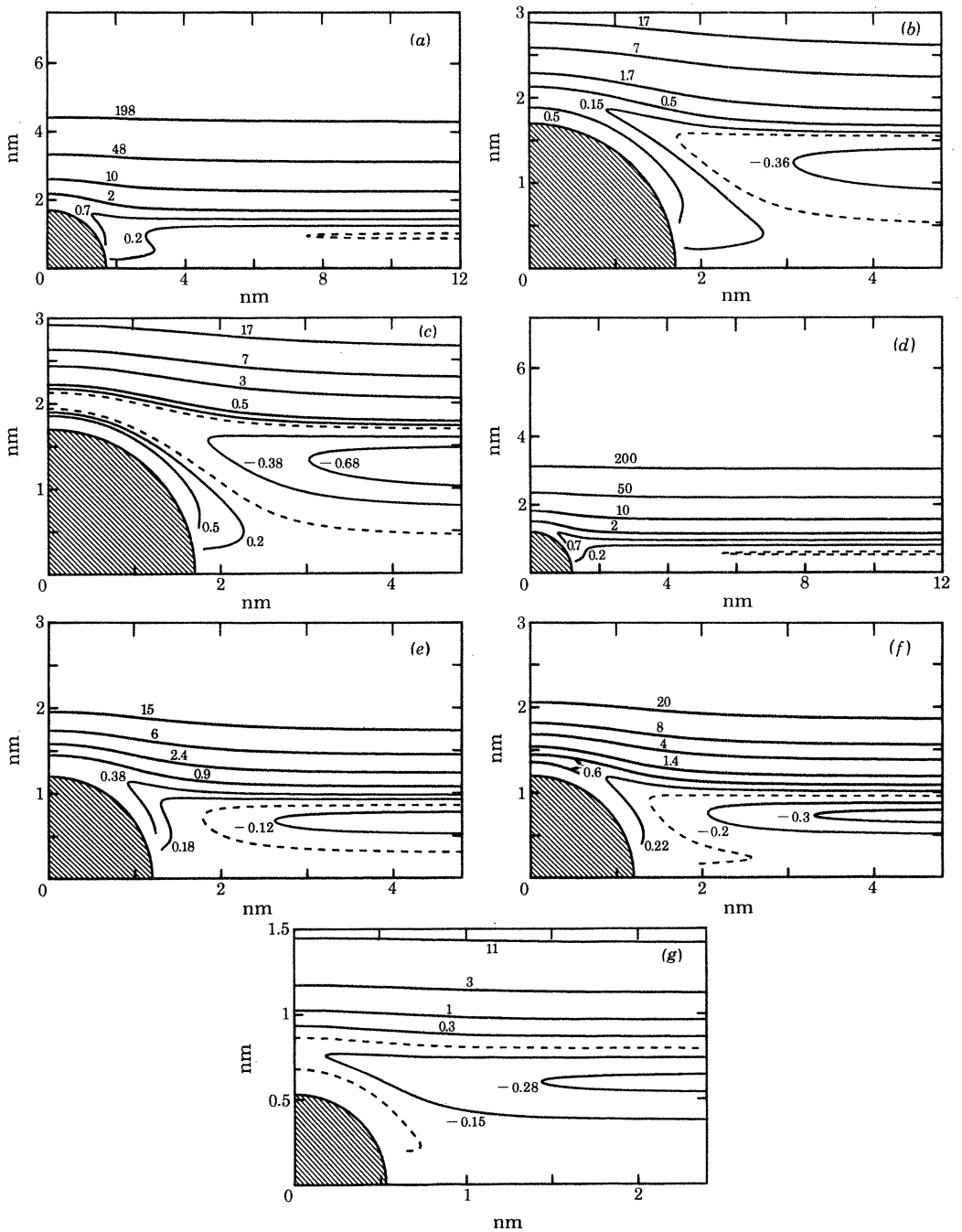

FIGURE 11. Contours of constant ΔE_R for encircling rings. Each graph is plotted on a plane through the centre of the ion and parallel to the initial ion-velocity U. The size and position of a vortex ring is specified by the point at which the ring crosses this plane. The axes represent distances from the centre of the ion. The figure against each curve is the value of $10^{21}\,\Delta E_R/\mathrm{J}$. The broken curve is the contour $\Delta E_R = 0$; (*a*) negative ions, pressure 0 Pa, $U = 56.3\ \mathrm{m\ s^{-1}}$; (*b*) negative ions, pressure 0 Pa, $U = 67\ \mathrm{m\ s^{-1}}$; (*c*) negative ions, pressure 0 Pa, $U = 72\ \mathrm{m\ s^{-1}}$; (*d*) negative ions, pressure 1.75×10^6 Pa, $U = 70.5\ \mathrm{m\ s^{-1}}$; (*e*) negative ions, pressure 1.75×10^6 Pa, $U = 79\ \mathrm{m\ s^{-1}}$; (*f*) negative ions, pressure 1.75×10^6 Pa, $U = 85\ \mathrm{m\ s^{-1}}$; (*g*) positive ions, pressure 0 Pa, $U = 110\ \mathrm{m\ s^{-1}}$.

However, we see also that our results for loops are relatively insensitive to the exact magnitude of the correction factors, and this gives us some confidence in the validity of our conclusions. Predicted critical velocities are changed by about 6 %. Furthermore, our conclusion that the nucleation of vortex loops is more favourable than that of encircling rings holds in all cases that we have investigated (including those in which no correction has been applied to either the energy or impulse, unless in this case δ, defined in (3.4.1), is rather less than 0.38 when nucleation of a very small ring near the pole of the ion may be favoured). Nevertheless, the possibility exists that the correction factors are totally wrong, in which case our conclusions would require modification. It is important to realize also that we have considered only two particular geometrical configurations of nucleating vortex, and the possibility cannot be ruled out that some other configuration is more favourable We believe, for example, that the loop of minimum energy is not strictly circular, but we guess that the resulting error is small.

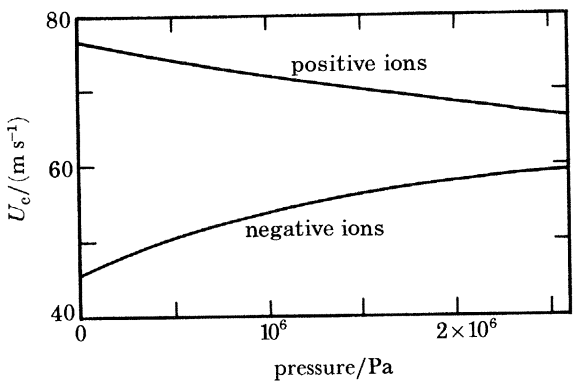

FIGURE 12. Predicted critical velocity, U_c, plotted against pressure for positive and negative ions.

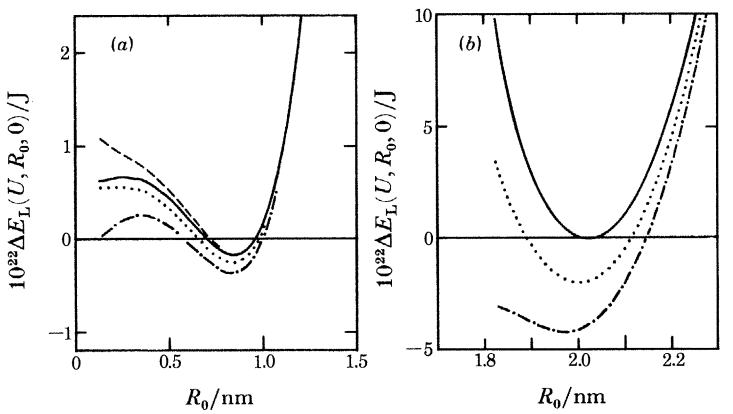

FIGURE 13. (*a*) ΔE_L $(U, R_0, 0)$ plotted against R_0 for $U = 46\ \mathrm{m\,s^{-1}}$ (negative ions, pressure = 0 Pa). (*b*) ΔE_R $(U, R_0, 0)$ plotted against R_0 for $U = 70\ \mathrm{m\,s^{-1}}$ (negative ions, pressure = 0 Pa).

Key: ——, with the full corrections described in § 3.4; – – –, with the corrections applied only to the energy; ....., with application of only half the energy correction (and no impulse correction in (*a*)); · – –, with no correction. (Note: Impulse corrections are negligible for rings of these radii.)

If the nucleating vortex forms at a true minimum of the energy ΔE_I, or ΔE_R, then the vortex will remain at rest relative to the ion (the ion having now a smaller velocity than the initial value U). Otherwise the vortex will move relative to the ion, the velocity of the ion changing to maintain a constant impulse. Tentatively, we might suppose that the vortex will move on one of

our calculated paths of constant energy at a rate proportional to the ratio of the magnitude of the local gradient in the energy to the length of vortex line. For the encircling rings, where the geometry has axial symmetry, this guess turns out to be correct (at least in the absence of the corrections discussed in §3.4), provided that effects associated with the finite effective mass of the vortex core can be neglected (these effects give rise to 'cyclotron' oscillations of the vortex, and we shall discuss them in the next section). For the loops, however, the time evolution is more complicated, because the loop becomes distorted; as we have already mentioned, we shall leave further discussion of this problem to a later paper, where we shall aim also to discuss time evolution of the vortex when the ion is subject to an accelerating electric field. It is interesting to note here, however, that if the distortion is ignored the vortex loop moves round one of the closed paths of constant energy shown in figure 10 in a time that turns out to be of order 10^{-10} s; the motion of the ion–vortex complex is therefore an oscillation of rather high frequency, the vortex following one of the paths of constant energy relative to the ion, and the ion oscillating relative to its time-averaged steady motion to conserve total impulse (again we neglect the cyclotron oscillations, which are generally superimposed on the vortex motion that we have just described).

4. Nucleation by quantum tunnelling

We have shown in §3 that nucleation of a vortex loop becomes energetically possible when the ion velocity exceeds a critical value, but that nucleation is impeded by a potential barrier. In the present section we shall discuss the possibility that nucleation can occur as the result of a direct quantum mechanical transition, which we shall interpret as involving a penetration of the barrier by quantum tunnelling. We shall suggest that such a process might well occur at a rate that is not inconsistent with the experimental facts. But we must make it clear that our discussion of this process will be tentative and speculative. Processes of this type have been discussed in the past by Volovik (1972), Sonin (1973) and Ichiyanagi (1976), but these authors did not take account of the effect of the finite mass of the vortex core on the dynamical behaviour of their systems.

A realistic calculation of the production of vortex loops by quantum tunnelling is difficult, and we do not know how to do it. We shall therefore attempt to solve a simpler problem that involves the same essential physics, and from which we can make a reasonable guess about the tunnelling rate for the vortex loops. This simpler problem relates to the nucleation of a vortex line at the edge of a thin flowing superfluid film at zero temperature.

We shall be concerned then with the possibility that a vortex can be created in a thin film by a tunnelling process. We shall regard the vortex as a particle that has both potential energy and kinetic energy. As we shall see in §4.1, the vortex behaves like a charged particle moving in a time-independent electromagnetic field, its mass being the effective mass, m_c, of the core of the vortex, and its potential energy being equivalent to the energy associated with the total velocity field in the superfluid. For vortex loops and rings this latter energy is just the one that we calculated in §3. (Strictly speaking this last statement requires some qualification. The energies calculated by Jones & Roberts (1982), on which we based the corrections described in §3.4, include the kinetic energy of the vortex core, evaluated for the case when the core moves with the local superfluid velocity (in general a core with finite effective mass does *not* move with this velocity). However, it can be shown that the resulting error is small and certainly less than the uncertainty in the magnitude of the corrections that we applied in §3.4.)

Our plan in the present part of the paper is as follows. First, in §4.1 we shall write down the

equations of motion of a vortex in a thin film, the core of the vortex having a finite effective mass, and we show that there is a useful electromagnetic analogy. In §4.2 we shall examine the quantum mechanics of the vortex, regarded as a particle, and we shall solve the appropriate wave equation in a situation that is relevant to the tunnelling problem. Then in §4.3 we shall deal with the nucleation of a vortex in a film, and finally in §4.4 we shall apply our results as best we can to the nucleation of vorticity by a moving ion.

4.1. *Equations of motion for vortices in a thin film: an electromagnetic analogy*

Let d be the thickness of the film and ρ_s the average superfluid density in the film. Each vortex has its axis normal to the plane of the film. The core of each vortex has an effective mass $m_c = md$; for a hollow core md is simply the mass of liquid displaced by the core (i.e. $m = \pi\rho_s a_0^2$). The equation of motion of such a vortex (circulation $\boldsymbol{\kappa}$) in a local velocity field $\boldsymbol{v}_s$ is

$$m\ddot{\boldsymbol{r}} = \rho_s(\boldsymbol{v}_s - \dot{\boldsymbol{r}}) \times \boldsymbol{\kappa}. \tag{4.1.1}$$

We have assumed that the vortex is subject only to a Magnus force and not to any frictional forces. We rewrite the equation of motion in the form

$$m\ddot{\boldsymbol{r}} = \rho_s\kappa\boldsymbol{v}_s \times \hat{\boldsymbol{\kappa}} - \rho_s\kappa\dot{\boldsymbol{r}} \times \hat{\boldsymbol{\kappa}}, \tag{4.1.2}$$

and compare it with that of an electrostatic line charge (q per unit length) attached to a line mass (m per unit length) moving in a direction normal to its length in an electromagnetic field ($\boldsymbol{E}$, $\boldsymbol{B}$); i.e. with

$$m\ddot{\boldsymbol{r}} = q\boldsymbol{E} + q\dot{\boldsymbol{r}} \times \boldsymbol{B}. \tag{4.1.3}$$

We see that there is an analogy if we take

$$q \equiv \kappa, \quad \boldsymbol{E} \equiv \rho_s \boldsymbol{v}_s \times \hat{\boldsymbol{\kappa}}, \quad \boldsymbol{B} \equiv -\rho_s\hat{\boldsymbol{\kappa}}. \tag{4.1.4)–(4.1.6}$$

Furthermore, the velocity field produced by the vortex itself, and the electric field produced by the line charge are also related by (4.1.5), so that the analogy also describes correctly the interaction between two vortices.

Vortices moving in a thin film are therefore equivalent in their behaviour to charged particles in a two-dimensional world moving in the steady electromagnetic field given by (4.1.5) and (4.1.6). In the particular case, which we discuss quantum-mechanically in the next section, of a vortex placed in an otherwise uniform flow at velocity U_s, the classical motion proves to be the superposition of a uniform translation of the core with velocity U_s and a uniform rotational motion of the core at (the cyclotron) angular frequency $\rho_s\kappa/m$ about a line parallel to the core but displaced from it. It follows straightforwardly from the electromagnetic analogy that the effective potential energy of the vortex is the field energy in the electric field, which is equivalent to the field energy in the velocity field $\boldsymbol{v}_s$.

4.2. *The quantum mechanics of a vortex in a thin film*

For reasons that will become clear in the next section, we shall discuss the quantum mechanics of a vortex (regarded as a particle moving in two dimensions) in the presence of an imposed uniform superfluid velocity, U_s, in the film. Using the results of §4.1, we can see that this situation is analogous to that of an electrostatic line charge (given by (4.1.4)) in a magnetic field given by (4.1.6) and an electric field given by

$$\boldsymbol{E} = \rho_s \boldsymbol{U}_s \times \hat{\boldsymbol{\kappa}}. \tag{4.2.1}$$

We work in Cartesian coordinates in which the z-axis is normal to the film (and therefore parallel

to the $\boldsymbol{B}$-field) and the x-axis is parallel to $\boldsymbol{E}$ (i.e. perpendicular to both $\boldsymbol{\kappa}$ and $\boldsymbol{U}_s$). If we choose a gauge in which the magnetic vector potential is $(0, Bx, 0)$, the wave equation for the vortex will then take the form

$$\frac{\partial^2\psi}{\partial x^2}+\left(\frac{\partial}{\partial y}+\frac{i\rho_s\kappa dx}{\hbar}\right)^2\psi+\frac{2md}{\hbar^2}\{\epsilon+\rho_s\kappa dU_s(x-b)\}\psi=0, \tag{4.2.2}$$

in exact analogy to that for a charged particle moving in crossed $\boldsymbol{E}$ and $\boldsymbol{B}$ fields. (We have chosen the scalar potential from which $\boldsymbol{E}$ is derived so that it is zero at $x = b$.)

To solve (4.2.2) we first put

$$\psi = e^{ik_y y}u(x) \tag{4.2.3}$$

and find that $u(x)$ is given by

$$\frac{d^2u}{dx^2}+\left\{\frac{2md\epsilon}{\hbar^2}+\frac{2\rho_s\kappa d^2mU_s}{\hbar^2}(x-b)-\left(k_y+\frac{\rho_s\kappa dx}{\hbar}\right)^2\right\}u=0. \tag{4.2.4}$$

Substituting

$$k_y' = k_y - mdU_s/\hbar, \tag{4.2.5}$$

we obtain

$$\frac{d^2u}{dx^2}+\left\{\frac{2md\epsilon}{\hbar^2}-\frac{2mdk_y'U_s}{\hbar}-\frac{2\rho_s\kappa d^2mU_sb}{\hbar^2}-\frac{m^2d^2U_s^2}{\hbar^2}-\left(k_y'+\frac{\rho_s\kappa dx}{\hbar}\right)^2\right\}u=0. \tag{4.2.6}$$

We see that this has the same form as the wave equation for the linear harmonic oscillator. We deduce that the eigenvalues are given by

$$\epsilon-\tfrac{1}{2}mdU_s^2-\rho_s\kappa dU_sb-\hbar k_y'U_s=(n+\tfrac{1}{2})\hbar\rho_s\kappa/m, \tag{4.2.7}$$

where n is an integer not less than zero. The eigenfunctions $u_n(x)$ will be harmonic oscillator eigenfunctions centred on a value of x given by

$$x_0 = -\hbar k_y'/\rho_s\kappa d, \tag{4.2.8}$$

and they will extend with large amplitude over a range of x given by $x_0 \pm r_0$, where r_0 (the radius of the cyclotron orbit in the electromagnetic analogue) is given by

$$r_0^2 \approx 2\hbar(n+\tfrac{1}{2})/\rho_s\kappa d. \tag{4.2.9}$$

The dependence of the wavefunction on y (equation (4.2.3)) implies that the vortex has a velocity in the y direction, given by

$$mdv_y = \hbar k_y + \rho_s\kappa dx. \tag{4.2.10}$$

If we put x equal to its mean value, x_0, for the vortex, we find that the mean velocity of the vortex in the y-direction is simply U_s. These quantum-mechanical results are clearly consistent with the known classical behaviour, as described at the end of the last section.

To deal with the tunnelling problem, we shall need to know how the function $u_n(x)$ behaves for values of x outside the range of the classical orbit, i.e. outside the range $x_0 \pm r_0$. Using the W.K.B. approximation we find that the required form of $u_n(x)$ is

$$u_n(x) \sim \exp\left[\left[\frac{-1}{\hbar}\int_{x_0\pm r_0}^{x}\left[2md\left\{\frac{\rho_s^2\kappa^2d}{2m}(x_0-x)^2-\left(n+\frac{1}{2}\right)\frac{\hbar\rho_s\kappa}{m}\right\}\right]^{\frac{1}{2}}\right]\right]dx; \tag{4.2.11}$$

i.e.

$$u_n(x) \sim \exp\left[\frac{-\rho_s\kappa d}{\hbar}\int_{x_0\pm r_0}^{x}\{(x_0-x)^2-r_0^2\}^{\frac{1}{2}}dx\right]. \tag{4.2.12}$$

where we have made use of (4.2.9).

4.3. *The nucleation of a vortex at the edge of a thin film by quantum tunnelling*

Let us now consider the production of a vortex line at the edge of a film in which there is a uniform superfluid velocity field U_s. We take the edge of the film to be the y-axis, and the velocity U_s is directed along the positive y-axis. If the vortex is formed at a distance x from the edge, the change in effective potential energy of the system is

$$\Delta V = \frac{\rho_s \kappa^2 d}{4\pi} \ln\left(\frac{2x}{a_0}\right) - \rho_s \kappa d x U_s, \tag{4.3.1}$$

provided that $x/a_0 \gg 1$; the corrections necessary when this inequality does not hold are of the type discussed in §3.4, and they do not alter the qualitative behaviour. The first term in (4.3.1) arises from the interaction of the vortex with its image; the second term from the interaction with the velocity field U_s. The form of ΔV as a function of x for $U_s = 40\ \mathrm{m\ s^{-1}}$ is shown in figure 14 We see that a potential barrier opposes the creation of the vortex. Vortex creation at the edge the film can take place at $T = 0$ only as a result of quantum tunnelling through this barrier.

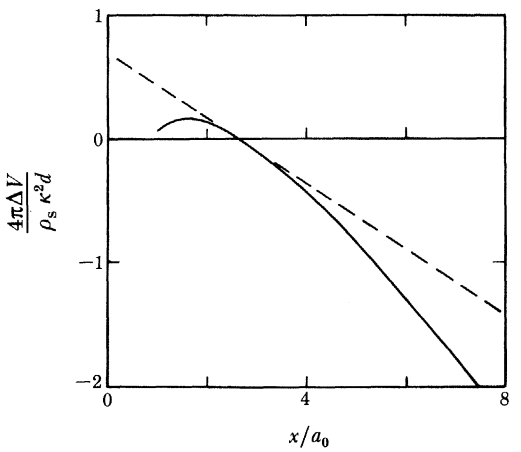

FIGURE 14. The effective potential energy ΔV of (4.3.1) plotted against x for $U = 40\ \mathrm{m\ s^{-1}}$. The broken line is a plot of the simplified expression (4.3.2).

To simplify the calculations we shall replace the real potential energy of the vortex by the form shown by the broken line in figure 14, which is given by

$$\Delta V = \rho_s \kappa d U_s'(w_0 - x), \tag{4.3.2}$$

where U_s' is an effective superfluid velocity (equal to about half U_s) and w_0 is the width of the potential barrier. We shall argue later that the change from (4.3.1) to (4.3.2) should have little effect on the results.

Strictly speaking, a film with an edge is not realistic, and we must be careful to define exactly the conditions that we imagine existing at this edge. We shall assume, initially, that the film is formed on a perfectly smooth substrate, and that it is bounded at its edge by a kind of two-dimensional solid wall. The vortex must then be formed as the result of an interaction that leads to an exchange of momentum between the helium and this wall. We presume that such an interaction can take place only if the wall is rough; i.e. has protuberances that destroy the translational invariance of the system in the direction parallel to the edge of the film.

The production of the vortex can now be considered by reference to figure 15. To conserve energy the total energy of the vortex must be zero, and it must be created in one of the states described in the preceding section. It will therefore be in a quantum state corresponding to an orbit with radius r_0 and centre x_0, the whole orbit moving in the y-direction with an average velocity U_s'. Suppose first that the wall contains a single localized protuberance, leading to a perturbation V acting on the helium. The resulting rate of production of vortices will be given by

$$\nu_0 = \frac{2\pi}{\hbar}\left|\int \psi_f^* V\psi_i \,\mathrm{d}\tau\right|^2 g(\epsilon), \tag{4.3.3}$$

where ψ_i and ψ_f are the initial (vortex free) and final (with vortex) states of the helium, and $g(\epsilon)$ is the final density of states associated with the vortex. The rate of vortex production depends therefore on the magnitude of the perturbation V, which is not known. However, we guess that a protuberance on a solid boundary will give rise to a strong perturbation, and that, furthermore, in the absence of the potential barrier such a perturbation will lead to vortex creation on a time-scale equal to the reciprocal of the 'cyclotron frequency', $\rho_s\kappa/m$, since this is the minimum time

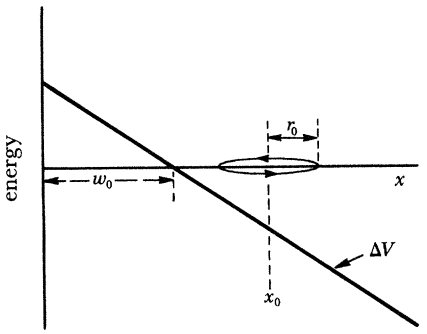

FIGURE 15. Diagram illustrating the nucleation of a vortex at the edge of a film by quantum tunnelling.

between the collisions of an orbiting vortex and a small fixed scattering centre. In the presence of the tunnelling barrier this rate will presumably be reduced by a factor of order the square of the extent to which the wavefunction of the vortex in its final state overlaps the perturbing protuberance on the wall, i.e. by the factor

$$\exp\left[-\frac{2\rho_s\kappa d}{\hbar}\int_0^{x_0-r_0}\{(x_0-x)^2-r_0^2\}^{\frac{1}{2}}\,\mathrm{d}x\right], \tag{4.3.4}$$

where we used (4.2.12). It follows that the rate of vortex production by the single perturbing protuberance will be given by

$$\nu_0 \sim \frac{\rho_s\kappa}{m}\exp\left[\frac{-2\rho_s\kappa d}{\hbar}\int_0^{x_0-r_0}\{(x_0-x)^2-r_0^2\}^{\frac{1}{2}}\,\mathrm{d}x\right]. \tag{4.3.5}$$

We remember now that the vortex must be formed with zero energy, so that x_0 and n must be related by the equation

$$x_0 = w_0 + (n+\tfrac{1}{2})\,\hbar/mdU_s + \frac{mU_s'}{2\rho_s\kappa}, \tag{4.3.6}$$

where we have used (4.2.7) and (4.2.8) with $\epsilon = 0$ and $b = w_0$. For values of w_0, d and U_s' that are comparable with analogous quantities for the ion problem, we find that

$$\hbar/mdU_s' \sim w_0 \quad \text{and} \quad mU_s'/2\rho_s\kappa \ll w_0. \tag{4.3.7), (4.3.8}$$

In making an approximate evaluation of (4.3.5) we can therefore first neglect tunnelling into states with $n > 0$, since such states would yield much smaller overlap integrals than those with $n = 0$, and secondly we can put

$$x_0 = w_0 + \hbar/2mdU_s'. \tag{4.3.9}$$

Furthermore, if $n = 0$, then $r_0^2 = \hbar/\rho_s \kappa d \ll w_0^2$. It follows that

$$\nu_0 \sim \frac{\rho_s \kappa}{m} \exp\left\{-\frac{\rho_s \kappa d}{\hbar}\left(w_0 + \frac{\hbar}{2mdU_s'}\right)^2\right\}. \tag{4.3.10}$$

This production rate refers to the effect of a single localized protuberance at the wall. If we assume that the wall is rough on an atomic scale, we can take the number of such protuberances per unit length of wall to be of order $1/a$, where a is an interatomic spacing, and we can assume further that the different protuberances act incoherently. It follows that the total rate of vortex production per unit length of wall will be given by

$$\nu = \frac{\nu_0}{a} \sim \frac{\rho_s \kappa}{ma} \exp\left\{-\frac{\rho_s \kappa d}{\hbar}\left(w_0 + \frac{\hbar}{2mdU_s'}\right)^2\right\}. \tag{4.3.11}$$

It turns out that, in situations comparable with those relevant to the ion problem, the rate ν does not depend strongly on the velocity U_s'; this is why we believe that the replacement of (4.3.1) by (4.3.2) will not have a serious effect. We remark in passing that for all practical cases of flow in a film, (4.2.11) seems to yield a negligibly small nucleation rate.

So far we have assumed that the substrate on which the film is formed is smooth. If it is not smooth, there could be two effects. First, there could be an added perturbation on the helium, leading to an increased nucleation rate. (This perturbation could also give rise to a different nucleation process – the creation of a vortex–antivortex pair – for which the wall is unnecessary.) Secondly, it could give rise to a frictional force opposing the motion of a vortex in the film. Such a force could decrease the nucleation rate (Caldeira & Leggett 1981). Suppose that the frictional force takes the form of a scattering process with relaxation time τ. If the results of Caldeira & Leggett still apply in the present situation, we would then expect the tunnelling rate to be reduced by a factor

$$\exp(-Amdw_0^2/\hbar\tau), \tag{4.3.12}$$

where A is a factor of order unity.

We recognize many possible defects in the arguments that we have been presenting. We have treated the vortex as a particle: in fact it has internal structure, so that, for example, there is not a unique path through the tunnelling barrier in the phase space of the helium. We have evaded the fact that strictly speaking the nucleation rate must depend on the exact strength of the perturbation at the walls of the helium, although in so doing we have probably introduced an error into only the prefactor in (4.3.11). Our treatment of the effect of friction may be in error, if we have made too naïve an application of the results of Caldeira & Leggett (1981).

4.4. *Application to nucleation of vorticity by a moving ion*

We cannot use the results of the preceding section to make quantitative predictions about vortex nucleation rates for moving ions, because the ion problem is essentially three-dimensional. However, the two-dimensional nucleation process that we have considered is not dissimilar in principle from that required for the ion, and therefore it seems reasonable to base a guess for the ion–vortex nucleation rate on the following modification of (4.3.10).

PHILOSOPHICAL TRANSACTIONS OF THE ROYAL SOCIETY A MATHEMATICAL, PHYSICAL & ENGINEERING SCIENCES

(i) We replace w_0 by the computed barrier width for the ion;

(ii) we take d equal to the length (roughly πw_0) of the tunnelling loop;

(iii) we take the prefactor to be of the order of the 'cyclotron' frequency, $\rho_s \kappa/m$, multiplied by the number of atoms on the surface of the ion. The results of this procedure are shown in table 1.

TABLE 1. PREDICTED VORTEX NUCLEATION RATES FOR NEGATIVE IONS AT $T = 0$

pressure/Pa	initial ion velocity/(m s^{-1})	nucleation rate/s^{-1}
0	46	7.84×10^{-64}
	52	2.92×10^{-11}
	56	7.15×10^{-3}
1.75×10^6	58	1.01×10^{-7}
	62	1.06×10^{4}
	66	9.22×10^{7}

When we come to compare our theory with experiment, in §7, we shall find that to date all observed nucleation rates relate to an ion that before nucleation is not travelling with constant velocity, as we have assumed in our theory, but is instead subject either to collisions with existing thermal excitations or to roton emission processes, the average velocity of the ion being maintained constant by means of an electric field. The most satisfactory experimental results relate to an ion for which vortex nucleation is accompanied by roton emission, this latter process occurring at a rate that is much larger than the vortex nucleation rate. As we mentioned in §2, it is important to know whether these two processes can be regarded as independent.

To answer this question tentatively we guess that the emission of a roton is equivalent to a scattering of the nucleating vortex, and therefore that the roton emission will reduce the vortex nucleation rate by the factor given in (4.3.12), where τ is now the average time interval between the emission of rotons. We shall discuss the consequences of this guess in §7.

It is interesting to note that in a quantum description of a vortex line, such as we are using in the present section, the core of the line is no longer necessarily localized in position. In the film problem the eigenstates described in §4.2 correspond to vortices that are completely delocalized in the direction parallel to the edge of the film. For vortex loops on an ion there will be a similar delocalization, with the result, for example, that a loop in the equatorial plane will be delocalized in the direction of changing azimuth.

5. NUCLEATION BY THERMAL EXCITATION

In this section we deal with briefly vortex nucleation by a moving ion at a finite temperature, where thermal excitation over the potential barrier can occur.

We recall from §3.5 that for a vortex loop the height of the potential barrier is typically 5×10^{-23} J, which corresponds to a temperature of about 3.6 K. It follows that thermal excitation over the barrier requires only the intervention of a single high-energy phonon or a single roton. Owing to the shape of the phonon–roton dispersion curve in helium, the density of rotons in thermal equilibrium always greatly exceeds the density of high-energy phonons, and therefore at a finite temperature we can expect a contribution to the nucleation rate that is proportional to the density of rotons. Furthermore, if nucleation involves the absorption of a roton, the

condition that the process conserve energy and momentum requires modification, and there is a resulting reduction in critical velocity. The details of this modification have been set out by Bowley *et al.* (1982) and need not be repeated here.

6. Comparison with the theoretical work of other authors

Detailed theoretical discussions of the nucleation of vorticity by a moving ion have been given previously by Donnelly & Roberts (1971) and Schwarz & Jang (1973). We comment briefly on the relation between this earlier work and our present treatment.

Donnelly & Roberts considered the nucleation of vortex loops by thermal activation. However, they assumed that at nucleation the velocity of the ion remains constant, so that they did not take proper account of the need to conserve energy and momentum. As we have already mentioned, the calculations of Schwarz & Jang are in the same spirit as our own, but these authors confined their attention to encircling rings, which turn out, if our own calculations are correct, to be not the most favourable nucleating geometry. Neither pair of authors considered the large corrections that we believe are necessary to the energy and impulse of the nucleating vortex when the ring or loop has a very small radius or is very close to the surface of the ion. We are not aware of any previous treatment of nucleation by quantum tunnelling.

7. A review of the experimental situation and a comparison with theory

7.1. *The experiments*

The experimental investigation of the nucleation of vortex rings from ions has proved to be a long and difficult task, full of subtle problems with a number of clever solutions. As we shall see there are few, if any, measurements in existence that directly address the theory contained in this paper. Furthermore, there are quite complete summaries of the literature in various publications over the years, particularly Careri (1961), Donnelly & Roberts (1971), Zoll (1976), Bowley *et al.* (1982). Nevertheless, a brief guide to some of the relevant experimental work on ion motion may be helpful to the reader.

The first indication that ion motion could be connected to vortex rings was reported by Meyer & Reif (1961). They discovered that ions at temperatures below 1 K failed to behave as they did at higher temperatures, and could not be stopped by simply reversing the potential gradient at some local position in the ion beam path. They named this phenomenon 'runaway behaviour'. Rayfield & Reif (1964) were able unambiguously to identify the runaway ions as charged quantized vortex rings. Meyer & Reif (1961) also observed that application of pressures above 1.5×10^6 Pa tended to inhibit ring production.

This early work stimulated a whole series of investigations by Careri *et al.* (1965), Rayfield (1966, 1967, 1968), Neeper (1968) and Neeper & Meyer (1969). These experiments showed that as the electric field $\mathscr{E}$ is increased, the average ion velocity $\bar{U}$ rises linearly at first, then approaches a maximum value V_c at $\mathscr{E} = \mathscr{E}_c$. For fields beyond $\mathscr{E}_c$, $\bar{U}$ decreased very rapidly (Careri named it the 'giant fall') and it was evident that the ions were dragging along vortex rings. It was observed that V_c lay in the region 30–50 m s^{-1} for either positive or negative ions for all pressures, and was relatively unaffected by temperature. A good discussion of this behaviour, and its modification by adding ^{3}He is contained in the paper by Zoll (1976), who has classified the various forms of

($\overline{U}, \mathscr{E}$) curves (cf. figure 1 of his paper). In particular, Zoll discusses the effects on the nucleation rates that result when pressure is applied to the negative ion and roton emission occurs simultaneously with ring creation.

Strayer & Donnelly (1971) reported a series of experiments in which $\overline{U}$ and signal currents were measured as a function of electric field $\mathscr{E}$. They demonstrated that the production of vortex rings is stochastic and the fraction of ions moving without vortex rings could be written

$$N/N_0 = \mathrm{e}^{-\bar{\nu}t}, \tag{7.1.1}$$

where N_0 is the number of ions in the bunch at $t = 0$.

Following Strayer & Donnelly (1971) were Titus & Rosenshein (1973), Zoll & Schwarz (1973) and Zoll (1976), who successively refined the techniques to measure $\bar{\nu}$ and $\overline{U}$. It became customary to define the critical velocity V_c as that value of $\overline{U}$ for which $\bar{\nu}$ takes a small but finite value (say $10^3\,\mathrm{s}^{-1}$). Some values of V_c for positive and negative ions at zero pressure are given in table 2.

TABLE 2. CRITICAL VELOCITIES AND THEIR PRESSURE DEPENDENCE

critical velocities for ions at $P = 0$

T/K	$V_c^+/(\mathrm{m\,s^{-1}})$	$V_c^-/(\mathrm{m\,s^{-1}})$	source
0.395	40.3	33.3	Zoll (1976)
0.60	37.9	32.2	Strayer (1971)
0.65	37.5	31.6	Strayer (1971)
0.70	37.0	31.0	Strayer (1971)
0.75	36.0	—	Strayer (1971)

pressure dependence of critical velocities at 0.65 K after Strayer (1971)

P/MPa	0	0.5	1	1.25	1.5
$V_c^+/(\mathrm{m\,s^{-1}})$	37.5	36.1	35.2	34.5	34.1
$V_c^-/(\mathrm{m\,s^{-1}})$	31.6	37.8	43.4	45.9	47.7

pressure dependence of critical velocities at 0.395 K after Zoll (1976)

P/MPa	0	0.5	1	1.5	2
$V_c^+/(\mathrm{m\,s^{-1}})$	40.1	37.1	—	35.9	
$V_c^-/(\mathrm{m\,s^{-1}})$	34.2	41.4	45.7	47.5	47.5

The more fundamental quantity is of course the transition rate $\bar{\nu}$ itself. Zoll & Schwarz (1976) were able to use an 'interrupted flight technique', which allowed them to measure $\bar{\nu}$ over four orders of magnitude: 10^2–$10^6\,\mathrm{s}^{-1}$. They also showed that the transition rate was nearly a universal function when plotted against $\mathscr{E}/\mathscr{E}_c$, where $\mathscr{E}_c$ is the field at which $\bar{\nu}$ becomes large. Figure 1 of their paper shows that such a plot tends to make results independent of temperature, pressure, ion species, and even ^{3}He concentration for the so-called 'typical' transition. A typical transition is one in which a large discontinuity in ion velocity occurs, indicating that when a vortex ring is formed it grows to large size before its drag comes into equilibrium with the applied field.

Zoll & Schwarz (1973) and Zoll (1976) pointed out that the ion velocities $\overline{U}$ reported are, of course, averages over a distribution of velocities, because the ions are continually colliding with excitations, the average velocity being kept constant by the field $\mathscr{E}$. The nucleation rate, ν, that we ourselves considered in earlier parts of our paper referred to ions moving before nucleation with a constant velocity U. We might hope that a calculation of $\nu(U)$ would give the instantaneous nucleation rate as a function of instantaneous ionic velocity, even when U is changing

with time, although this may not be so, as is clear from our discussion in §4.4 of the possible effect of roton emission on nucleation rate. However, to calculate $\bar{\nu}(\bar{U})$ from a knowledge of $\nu(U)$ (or vice versa) requires at least a knowledge of the ionic velocity distribution function, which is not generally available. That this is a major problem can be seen when it is realized that the spread in ionic velocities is typically a few metres per second, within which ν could change by several orders of magnitude. The most satisfactory remedy would be to do experiments at temperatures sufficiently low that collisions with excitations can be ignored, but there are formidable problems in controlling ionic motion under these conditions.

The most recent and most extensive set of measurements on ion–vortex nucleation have addressed this problem in a different way. They come from McClintock and his colleagues at Lancaster University and span nearly a decade of systematic research. The approach of this group was to go back to the early observation of Meyer & Reif (1961) that application of pressure above 1.5×10^6 Pa quenched ring production for negative ions. Application of pressure changes the radius of the negative ion (Springett & Donnelly 1966), reduces the roton gap Δ (Brooks & Donnelly 1977) and hence reduces the Landau critical velocity for roton emission below the ion nucleation threshold. The Lancaster nucleation studies, then, are entirely devoted to negative ions at elevated pressures, where roton emission and nucleation are competing processes. A potential advantage is that the distribution function of velocities in the presence of roton emission is known theoretically (Bowley & Sheard 1977), so that some progress can be made in extracting $\nu(U)$ from the observed $\bar{\nu}(\bar{U})$. There remains, however, the problem of whether roton creation and vortex nucleation are independent processes. Another development was a new method for measuring $\bar{\nu}$ based on electrostatic induction, which allows electric fields to be employed two orders of magnitude greater than used previously. Thus $\bar{U}$ could be extended beyond V_c.

Perhaps the greatest surprise from the experimental point of view was the discovery by the Lancaster group that even the concentration of ^{3}He present in helium gas from wells is enough to alter $\bar{\nu}$ profoundly (Bowley *et al.* 1980). This discovery casts doubt on the significance of all earlier nucleation studies, including those quoted in table 2. Indeed a comparison of the results of Bowley *et al.* with those of earlier workers suggests that the critical velocities quoted in table 2 may have been reduced by as much as $10\,\mathrm{m\,s^{-1}}$ by the effect of ^{3}He.

Measurements of $\bar{\nu}(\mathscr{E}, P, T)$ together with $\bar{U}(\mathscr{E})$ are reported in detail by Bowley *et al.* (1982) for negative ions in purified ^{4}He in the range of pressure (P) from 1.5×10^6 to 2.5×10^6 Pa, of temperature (T) from 0.3 to 0.87 K, and electric field up to $10^6\,\mathrm{V\,m^{-1}}$. For a given pressure and field they find that $\bar{\nu}$ is essentially independent of temperature below 0.5 K and increases rapidly at higher temperatures. For a fixed pressure the experimental results are found to be consistent with a relation of the form

$$\bar{\nu}(\bar{U}, T) = \bar{\nu}_s(\bar{U}) + n_r\,\bar{\nu}_r(\bar{U}), \tag{7.1.2}$$

where the first term on the right side is independent of temperature, while the second is proportional to the density n_r of rotons.

Bowley *et al.* (1982) are not able unambiguously to deduce the form of $\nu(U)$ from the observed form of $\bar{\nu}(\bar{U})$. They show, however, that if $\nu_s(U)$ has the form

$$\left.\begin{aligned} &\nu_s = 0, && U < v_1 \quad \text{or} \quad U > v_3,\\ &\nu_s = R_1, && v_2 > U > v_1,\\ &\nu_s = R_1 + R_2, && v_3 > U > v_2, \end{aligned}\right\} \tag{7.1.3}$$

then the parameters R_1, R_2, v_1, v_2, v_3 can be chosen to give a good fit to the observed form of $\bar{\nu}_s(\bar{U})$, when (7.1.3) is combined with the known ionic velocity distribution function. The required values of the parameters are summarized in table 3. The precise form (7.1.3) of the dependence of ν_s on U has no significance (a smoother variation would presumably be more reasonable and could, as we understand it, be made to fit the experimental results equally well), but it is nevertheless significant that ν_s does not seem to increase as rapidly with U, in the range $v_1 < U < v_3$, as one might have expected from our theory of §4.4, and that, surprisingly, ν_s actually falls at the highest velocities. The form of $\nu_r(U)$ proves to be similar to that of $\nu_s(U)$, but the critical velocity v_1 is reduced.

TABLE 3. NUMERICAL VALUES OF THE PARAMETERS USED BY BOWLEY *et al.* (1982) IN FITTING (7.1.3) TO THEIR LOW-TEMPERATURE VORTEX NUCLEATION DATA

pressure/MPa	1.7	1.9	2.1	2.3	2.5
$10^{-3}\,R_1/\mathrm{s}^{-1}$	23	12.3	4.7	2.6	1.8
$10^{-3}\,R_2/\mathrm{s}^{-1}$	195	146	150	95	56
$v_1/(\mathrm{m\,s}^{-1})$	59.8	59.3	59.8	60.7	60.6
$v_2/(\mathrm{m\,s}^{-1})$	69.8	69.1	69.8	69.9	70.1
$v_3/(\mathrm{m\,s}^{-1})$	72	71.4	71.3	71.7	71.7

7.2. *Comparison with theory*

In comparing the results of our theoretical study with experiment, we note first that the theory is consistent with the observation that the nucleation process is stochastic in nature (equation (7.1.1)).

Before we can proceed further we must remember that, as we have already emphasized, the nucleation process has been observed to be seriously affected by the presence of small (even naturally occurring) amounts of ^{3}He. We intend to discuss this effect in a later paper. For the present, however, we must accept that, in looking for experimental results that we can use in a quantitative comparison with theory, we are limited to the most recent work of Bowley *et al.* (1982). As we have seen, this work did relate to purified ^{4}He, but it was confined to conditions of high pressure, where vortex nucleation competes with roton emission.

Let us first assume that vortex nucleation and roton emission occur independently. The observation of Bowley *et al.* (1982) that at the lowest temperatures the vortex nucleation rate, ν_s, becomes independent of temperature is consistent with our suggestion that quantum tunnelling occurs in these circumstances. Their suggested form of the dependence of ν_s on instantaneous ion-velocity, U (equation (7.1.3)), leads us to identify their v_1 with our critical velocity U_c, and we see that there is satisfactory agreement; but the fact that ν_s appears not to increase very rapidly with velocity, and more seriously, that ν_s actually falls at the higher velocities is not apparently consistent with our theory (compare tables 1 and 3). The behaviour at higher temperatures, when a nucleation process depending on the absorption of a roton is observed, is, however, consistent with our own results of §6.

There remains the problem arising from the observed decrease in ν at high velocities (or high electric fields). Our theory does not support the view of Bowley *et al.* (1982) that this effect is evidence that vortex nucleation involves the direct creation of encircling rings. As we mentioned in §2, it does nevertheless seem possible that a loop might evolve into a ring and then be cast off from the ion (or be cast off in some other way); and we aim to examine this idea in a later paper.

However, our discussion in §4.4 suggests that the fall in ν at high velocity might possibly have a quite different explanation, which is related to the important question of whether or not vortex nucleation and roton emission can occur independently. We have made the tentative suggestion that roton emission will reduce the rate of vortex nucleation by the factor given in (4.3.12), where $1/\tau$ is put equal to the rate of emission of rotons (strictly speaking, roton pairs; see Allum *et al.* (1977)). Consider, for example, the observed nucleation rate at a pressure of 1.7×10^6 Pa. We find from the paper of Bowley *et al.* (1982) that the vortex nucleation rate starts to fall for electric fields greater than about $7 \times 10^5\,\mathrm{V\,m^{-1}}$. This field corresponds to a rate of emission of roton pairs of about $2.7 \times 10^{10}\,\mathrm{s^{-1}}$; if we take $d/\pi = w_0 = 3 \times 10^{-10}$ m and, as before, $m = \pi\rho_s a_0^2$, we find that this situation corresponds to a value of $mdw_0^2/\hbar\tau \approx 0.26$, which is of order unity. Now if the factor $Amdw_0^2/\hbar\tau$ is less than a value of order unity, then we expect the vortex nucleation rate to be relatively unaffected by roton emission; however, if the same factor becomes significantly larger than unity we expect the vortex nucleation rate to be drastically reduced. Given the uncertainty in the value of the parameter A, we see that the fall off in the nucleation rate at the high fields observed by Bowley *et al.* (1982) might well arise from an increasing interference from the roton emission. However, it must be added that the experiments indicate a fall off affecting not only the temperature-independent part of the vortex nucleation rate, but also the temperature-dependent part, and it is not obvious that the factor given in (4.3.12) should play any role in the thermally activated process.

Our attempt to compare the results of our theory with experiment draws attention to a serious shortage of experimental data. At present there exist no measurements of vortex nucleation rates in pure ^{4}He at low pressures. Furthermore, there exist no measurements of these rates under conditions where the ion motion is not perturbed, perhaps seriously, by either roton emission or collisions with existing excitations. This type of perturbation may have a particularly serious effect on nucleation by quantum tunnelling, and we emphasize that our own discussion of this effect is speculative and quite possibly wrong. The satisfactory comparison with experiment of theories of vortex nucleation by a moving ion in superfluid ^{4}He must therefore await further experimental work, and we hope that the present paper will encourage the development of such work.

8. Conclusions

We have developed a theory of vortex nucleation by a moving ion in superfluid ^{4}He. Our calculations show that the vortex nucleus is probably a loop out of the side of the ion, and they confirm that the nucleation process tends to be inhibited by a potential barrier, but an accurate calculation is not possible in the absence of detailed and realistic theories both of the core structure of a quantized vortex line and related matters, such as the behaviour of very small vortex rings and their interaction with a nearby boundary. We have presented a first tentative theoretical discussion of the possibility that nucleation takes place by a direct quantum mechanical transition involving penetration of the barrier by quantum tunnelling, and we have suggested that such a process might well take place at an observable rate at the lowest temperatures. At higher temperatures thermal excitation over the barrier ought to be possible by absorption of a single roton. We have commented tentatively on the way in which roton emission (or collisions with existing excitations) might interfere with nucleation by quantum tunnelling. We have compared the results of our discussion with experiment; there is some pleasing agreement, but many mor

experiments, some of a type not so far attempted, would be required to provide a proper test of the theory.

After this paper had been written we learned of work by R. M. Bowley (to be published) that is based in part on the ideas that we have presented. However, Bowley's approach differs from ours in a number of important ways, and we intend to discuss these differences in a later paper.

We are very grateful to Dr R. M. Bowley, Dr P. V. E. McClintock, Dr P. C. E. Stamp, and Dr N. Thomas for helpful and stimulating discussions, and to Professor P. H. Roberts, F.R.S., and Dr C. A. Jones for showing us their work before publication and for performing some extra computations. Our work has been supported by a grant (DMR 81–17570) from the National Science Foundation Low Temperature Physics Program, as well as a travel grant from the U.S.–U.K. International Program of the National Science Foundation.

References

Allum, D. R., McClintock, P. V. E., Phillips, A. & Bowley, R. M. 1977 *Phil. Trans. R. Soc. Lond.* A **284**, 179–224.
Blood, F. A. 1976 *Physics Fluids* **19**, 1435–1438.
Bowley, R. M., McClintock, P. V. E., Moss, F. E., Nancolas, G. G. & Stamp, P. C. E. 1982 *Phil. Trans. R. Soc. Lond.* A **307**, 201–260.
Bowley, R. M., McClintock, P. V. E., Moss, F. E. & Stamp, P. C. E. 1980 *Phys. Rev. Lett.* **44**, 161–164.
Bowley, R. M. & Sheard, F. W. 1977 *Phys. Rev.* B **16**, 244–254.
Brooks, J. S. & Donnelly, R. J. 1977 *J. phys. Chem. ref. Data* **6**, 51–104.
Caldeira, A. O. & Leggett, A. J. 1981 *Phys. Rev. Lett.* **46**, 211–214.
Careri, G. 1961 *Progress in low temperature physics* (ed. G. J. Gorter), vol. 3, pp. 58–79. Amsterdam: North–Holland.
Careri, G., Cunsolo, S., Mazzoldi, P. & Santini, M. 1965 *Phys. Rev. Lett.* **15**, 392–396.
Donnelly, R. J. & Roberts, P. H. 1971 *Phil. Trans. R. Soc. Lond.* A **271**, 41–100.
Ellis, T., McClintock, P. V. E. & Bowley, R. M. 1983 *J. Phys.* C. **16**, L485–489.
Ellis, T., McClintock, P. V. E., Bowley, R. M. & Allum, D. R. 1980 *Phil. Trans. R. Soc. Lond.* A **296**, 581–595.
Fetter, A. L. 1971 *Phys. Rev. Lett.* **27**, 986–992.
Fetter, A. L. 1976 In *The physics of liquid and solid helium* (ed. K. H. Bennemann & J. B. Ketterson), part 1, ch. 3. New York: J. Wiley.
Glaberson, W. I. 1969 *J. low Temp. Phys.* **1**, 289–311.
Ichiyanagi, M. 1976 *J. low Temp. Phys.* **23**, 599–603.
Jones, C. A. & Roberts, P. H. 1982 *J. Phys.* A **15**, 2599–2619.
Lamb, H. 1952 *Hydrodynamics*. New York: Dover Publications.
Landau, L. D. 1941 *J. Phys., Moscow* **5**, 71–90.
Meyer, L. & Reif, F. 1961 *Phys. Rev.* **123**, 727–731.
Neeper, D. A. 1968 *Phys. Rev. Lett.* **21**, 274–275.
Neeper, D. A. & Meyer, L. 1969 *Phys. Rev.* **182**, 223–224.
Norbury, J. 1973 *J. Fluid Mech.* **57**, 417–431.
Phillips, A. & McClintock, P. V. E. 1974 *Phys. Rev. Lett.* **33**, 1468–1471.
Rayfield, G. W. 1966 *Phys. Rev. Lett.* **16**, 934–936.
Rayfield, G. W. 1967 *Phys. Rev. Lett.* **19**, 1371–1373.
Rayfield, G. W. 1968 *Phys. Rev.* **168**, 222–223.
Rayfield, G. W. & Reif, F. 1964 *Phys. Rev.* A **136**, 1194–1208.
Schwarz, K. W. & Jang, P. S. 1973 *Phys. Rev.* A **8**, 3199–3210.
Sonin, E. B. 1973 *Soviet Phys. JETP* **37**, 494–500.
Springett, B. E. & Donnelly, R. J. 1966 *Phys. Rev. Lett.* **17**, 364–367.
Steingart, M. & Glaberson, W. I. 1972 *J. low Temp. Phys.* **8**, 61–77.
Strayer, D. M. 1971 Ph.D. thesis, University of Oregon.
Strayer, D. M. & Donnelly, R. J. 1971 *Phys. Rev. Lett.* **26**, 1420–1423.
Strayer, D. M., Donnelly, R. J. & Roberts, P. H. 1971 *Phys. Rev. Lett.* **26**, 165–169.
Takken, E. H. 1970 *Phys. Rev.* A **1**, 1220–1239.
Titus, J. A. & Rosenshein, J. S. 1973 *Phys. Rev. Lett.* **31**, 146–149.
Vinen, W. F. 1963 In *Liquid helium: Proc. International School of Physics Enrico Fermi*, course XXI, pp. 336–355. New York: Academic Press.
Volovik, G. E. 1972 *Soviet Phys. JETP Lett.* **15**, 81–83.
Zoll, R. 1976 *Phys. Rev.* B **14**, 2913–2926.
Zoll, R. & Schwarz, K. W. 1973 *Phys. Rev. Lett.* **31**, 1440–1443.

PHILOSOPHICAL TRANSACTIONS OF THE ROYAL SOCIETY A MATHEMATICAL, PHYSICAL & ENGINEERING SCIENCES